The promise of 3C 3D seismic data for improved imaging and reservoir characterization in the Alberta oil sands

Bobby J. Gunning, Don C. Lawton and Helen Isaac

ABSTRACT

A 3D 3C seismic data set from the Athabasca Oil Sands region was processed and interpreted. The vertical and radial geophone components were processed as the PP and PS seismic data. PP and PS seismic data were processed to stack using Vista and ProMAX processing software. Prestack PP gathers were generated for analysis. Stacked datasets were correlated with regional well control and pervasive reflection horizons were picked. The main hydrocarbon reservoir, the McMurray formation was studied based on the PP and PS seismic datasets. A large Upper McMurray aged channel feature was found running through the seismic volume. Truncations of regional seismic character were found at the McMurray channel location. A model-based post stack impedance inversion is performed on the PP seismic data. Interval RMS amplitude and impedance reveal in-situ natural gas and higher quality reservoir; these findings are correlated with geological control. A model-based pre-stack inversion was performed. The pre-stack inversion P impedance volume showed better differentiation of regional McMurray units than the post stack inversion.

INTRODUCTION

Introduction

The projected growth of the hydrocarbon extraction industry in Alberta is heavily weighted in the bituminous sand deposits. By 2030, 1.8 million bbl/day will be added to oil sands production (CAPP, 2015). Multicomponent seismic reflection data is useful for understanding the subsurface geology. The benefits of collecting and processing both the PP and PS reflections for improved reservoir understanding is studied in this paper. A recently acquired commercial seismic volume acquired in Northeast Alberta was processed and interpreted. No contemporary drilling or production activity is occurring in the study area. Both the PP and PS seismic volumes have been processed to stack. Pre-stack gathers have also been output for AVO analysis. The stacked datasets have a high signal to noise ratio, conducive to detailed geological interpretation. The PP pre-stack gathers have relatively high signal to noise ratio, however the PS pre-stack gathers have more limited interpretability. Regional interpretations have been completed for the stacked datasets. Seismic stratigraphy, regional structure and potential hydrocarbon sweet spots have been identified through joint PP-PS interpretation. The main interpretation techniques utilized include: horizon mapping, structure mapping, amplitude mapping and isochron analysis. Post-stack and pre-stack joint and individual inversions have provided several sources of rock physics volumes. The inversion techniques are high-graded based on their ability to predict well data.

The dataset

A recent 3D 3C oil industry seismic line, covering an area of 17 km^2 in the Athabasca Oil Sands is used in this study. The data were collected using a dynamite source with orthogonal acquisition geometry. Source lines, oriented East-West, had 125 m spacing and

reciever lines, oriented North-South, also had 125 m spacing. Sources and receivers were placed at 25 m intervals, generating a 12.5 x 12.5 m natural bin size. Some source locations had hazards in the vicinity and could not be acquired. Figure 1 depicts the source and reciever geometry. The live patch consisted of 648 channels, with a centered source.

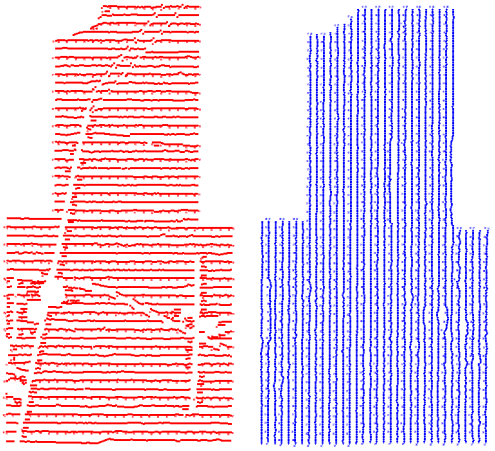

FIG. 1. Source (left) and receiver (right) line geometry.

Well log data from 14 wells was available for use in this study. All of the wells have sonic and density logs, and 4 of the wells have dipole sonic logs, 3 of which are within the seismic suvery and one 500 m outside of the survey. Most of the wells have additional logs including: caliper, resistivity, gamma ray, neutron porosity and photoelectric effect.

Geological setting

An intense history of hydrocarbon exploration and production has been conducive to a solid understanding of the subsurface in Northeast Alberta. Conventional and unconventional oil and gas plays have been targetted for several decades. There are three major sedimentary sequences which play a role in this part of the basin. The Paleozoic carbonates and shales make up the oldest sedimentary component, on top of which the Cretaceous clastics lie. Within the Cretaceous clastics are the major oil sands reservoirs and their corresponding caprock. The overburden is Quaternary glacial till and fluvial sediments. A generalized stratigraphic chart is shown in Figure 2.

The base reservoir, and oldest unit of interest for this study, is the Devonian Beaverhill Lake Group. The Cretaceous-Devonian boundary is an angular unconformity with a very mild dip. The Beaverhill Lake Group dips at 0.4 degrees (Oldale and Munday, 1994). The unit is made up of predominantly carbonates and to a lesser extent, shales and evaporites. The Cretaceous-Devonian unconformity displays variable topography which influences the structure and isopach of younger units. Directly above the Paleozoic, lies the McMurray Formation of the Manville Group. The McMurray is the main target for oil sands development in the Athabasca Oil Sands. The McMurray is usually split into Upper and Lower sequences. The Lower McMurray is more fluvial, with complex channel and point bar facies. The Upper McMurray is split again into McMurray A and B sequences, which are again split into finer detail. The Upper McMurray contains brackish water ichofossils and has a more marine characeter, usually interpretted as a low enrgy shoreface or small

deltaic system (Gingras and Rokosh, 2004). The remaining sands and shales of the Manville Group act as a cap rock for thermal operations in the McMurray Formation. The Clearwater Formation conformably overlies the McMurray. The Wabiskaw Member, a fine-grained, well sorted glauconitic sandstone with interbedded shales acts as a secondary target for oil sands extraction (Glass, 2009). The remainder of the Clearwater Formation is a marine shale. The uppermost unit of the Manville Group is the Grand Rapids Formation. The Grand Rapids is a series of coarsening upward shoreface sequences with incised valley fills (Leckie et al, 1994). The Cretaceous Colorado group, which is bounded above and below by unfornmormities, lies above the Manville. The Colorado Group is made up of almost entirely low permeability mudstones. The overburden in the Athabasca region is made up of unconsolidated glacial and fluvial sediments, deposited in the Quaternary. These drift sequences can be over 300 m thick in places (Andriashek, 2003).

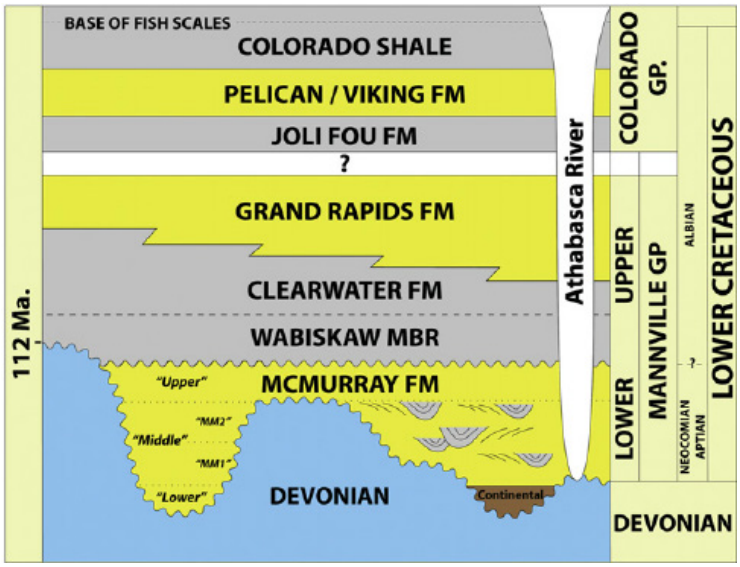

FIG. 2. Stratigraphy in the Athabasca Oil Sands (Todorovic-Marinic et al. 2015).

Specifically within the project area, the main reservoir facies are fairly well understood. A component of the regional McMurray sequence is eroded away by a large McMurray B age channel fill. In some regions the McMurray B channel fill erodes almost entirely through the Lower McMurray (McMurray C) and to the Paleozoic Unconformity. Another regionally anomalous geological feature in the project area is a large Wabiskaw age valley-fill deposit. This feature erodes into the Upper McMurray. Both the McMurray B channel fill and the Wabiskaw channel fill are considered good reservoirs.

VERTICAL AND CONVERTED WAVE PROCESSING

Processing was done jointly between the PP and PS seismic data. Geologically, the main interval of interest extends from the surface to the Paleozoic Unconformity (Devonian Beaverhill Lake Group). The Cretaceous-Devonian contact has a large P and S acoustic impedance contrast, generating high amplitude reflections that appear on both the PP and PS seismic datasets. This bright reflection is at approximately 500 ms and 1200 ms on the raw PP and PS volumes respectively.

The raw horizontal component records were rotated into radial and transverse components (Figures 3, 4 and 5). The vertical geophone component dominantly records compressional waves; the radial and transverse components record shear waves. The most obvious features on all 3 raw records are ground roll and refracted arrivals. Hyperbolic reflection events are present and fairly obvious on the PP raw record (Figure 3). Reflection hyperbolas are visible on the radial shot gather (Figure 4), being most visible are the largest offsets. No easily distinguishable reflection events are visible on the transverse shot gather (Figure 5). The fact that converted wave reflections are limited to the radial shot gather may imply that the subsurface is isotropic or vertical transverse isotropic. There is no immediate evidence of shear wave birefringence. Using this assumption, converted wave processing was limited to dominantly the radial geophone component at this time.

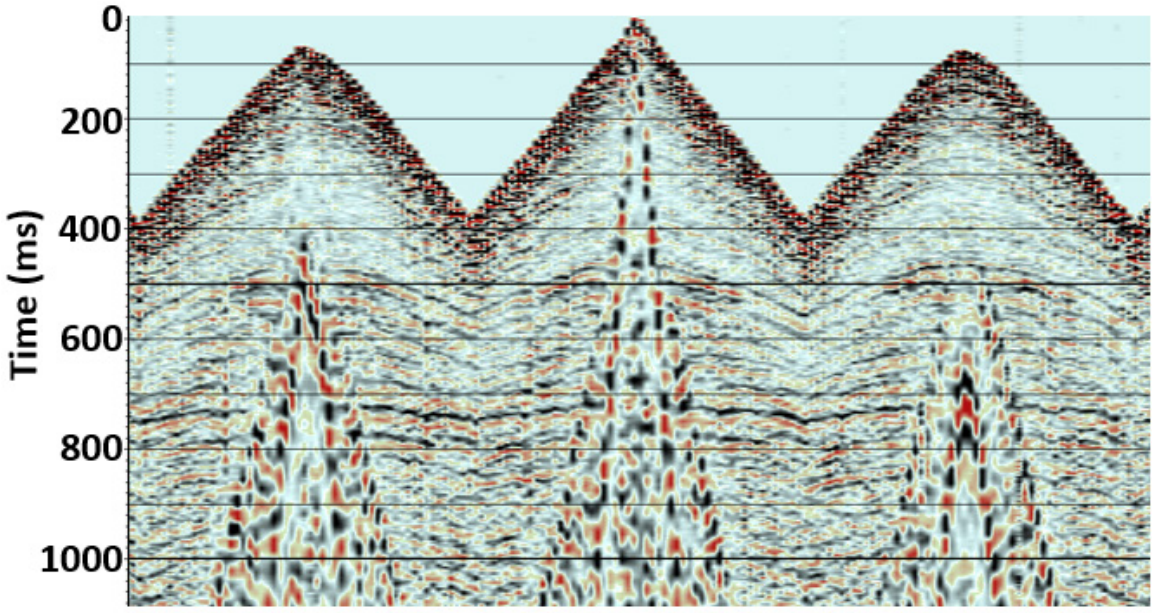

FIG. 3. Sample vertical shot record.

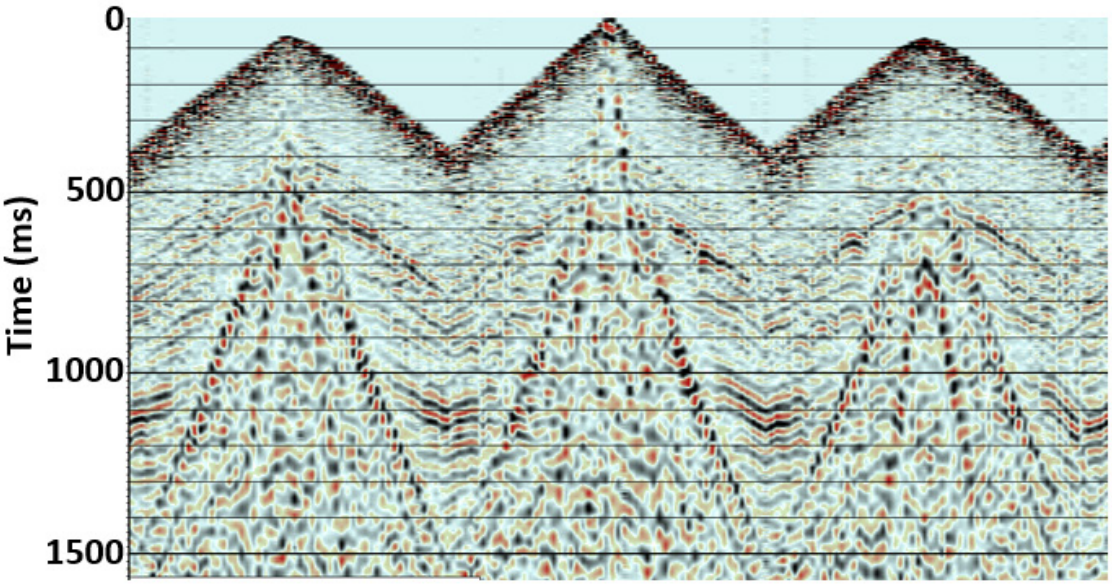

FIG. 4. Sample radial shot record.

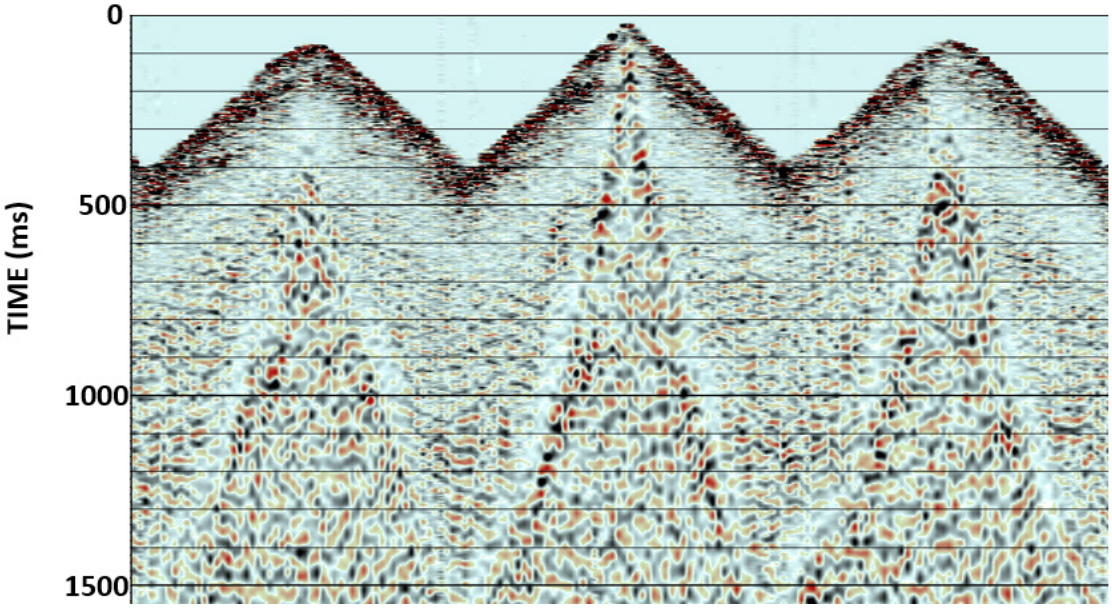

FIG. 5. Sample transverse shot record.

PP Processing

The vertical component was processed into several output volumes following a conventional 3D processing flow. Full offset stack, near offset stack, mid offset stack, far offset stack and pre-stack gathers were generated. The first step in processing is geometry assignment and binning. The orthogonal acquisition geometry and 25 m source and receiver spacing produces a natural binning grid with 12.5 m by 12.5 m cells. Following geometry and binning, elevation and receiver statics were calculated and applied. Variable topography was corrected for by applying elevation statics. A datum of 750 m and a replacement velocity of 1900 m/s was used. Surface elevation in the project area did not change significantly, but there was still some variability. The topography ranged from a

minimum of 660 m to a maximum of 690 m. Refraction statics were calculated from first break time picks. A scatterplot of time versus offset for first break picks shows two slopes (Figure 6), indicating two near surface low velocity layers. P wave Refraction velocities in the first layer are around 1600 m/s and refraction velocities in the second layer are around 2000 m/s. Isaac (1996), in a similar geological regime, found refraction velocities ranging from 1750 – 1800 m/s using a single low velocity layer assumption. Our refraction velocities are relatively close to those found by Isaac (1996). Refraction statics for the PP processing ranged from 15 to 30 ms.

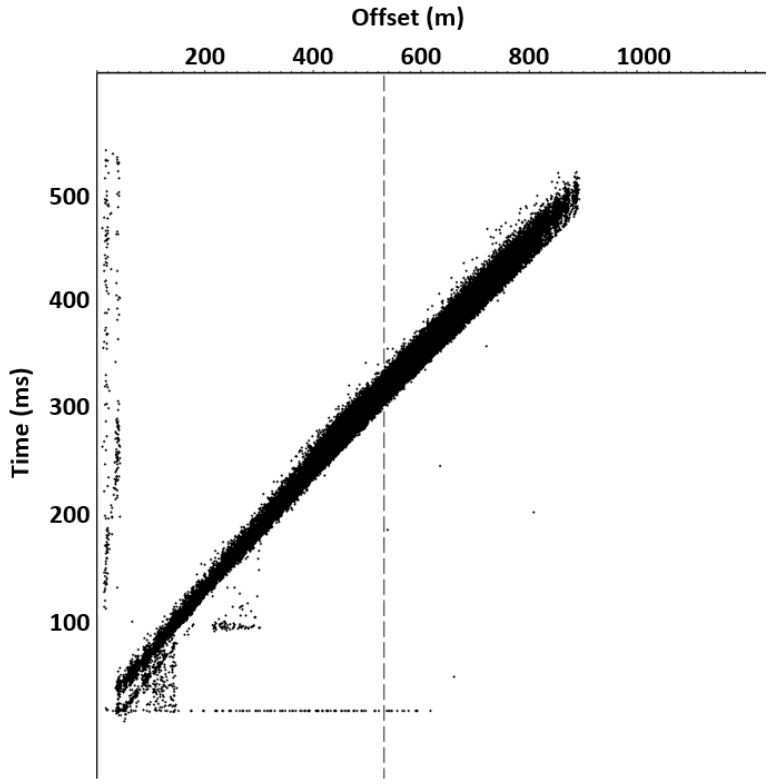

FIG. 6. Scatterplot of first break times versus offset, dotted line indicated the point at which the slope changes.

After the application of elevation and refraction statics, a radial transform denoise algorithm was implemented to attenuate the coherent ground roll noise. Figure 7 shows an example radial transform of a shot gather including the ground roll. To remove ground roll from the radially transformed shot gather, a low cut filter is used. Amplitude corrections were made next. Exponential gain corrects the effects of geometric spreading and mean scaling trace balance. Gabor deconvolution, a non-stationary deconvolution technique was used to enhance frequency. Before and after Gabor deconvolution images are shown in Figure 8. In addition to Gabor deconvolution, time-variant spectral balancing is applied to whiten each trace's amplitude spectrum.

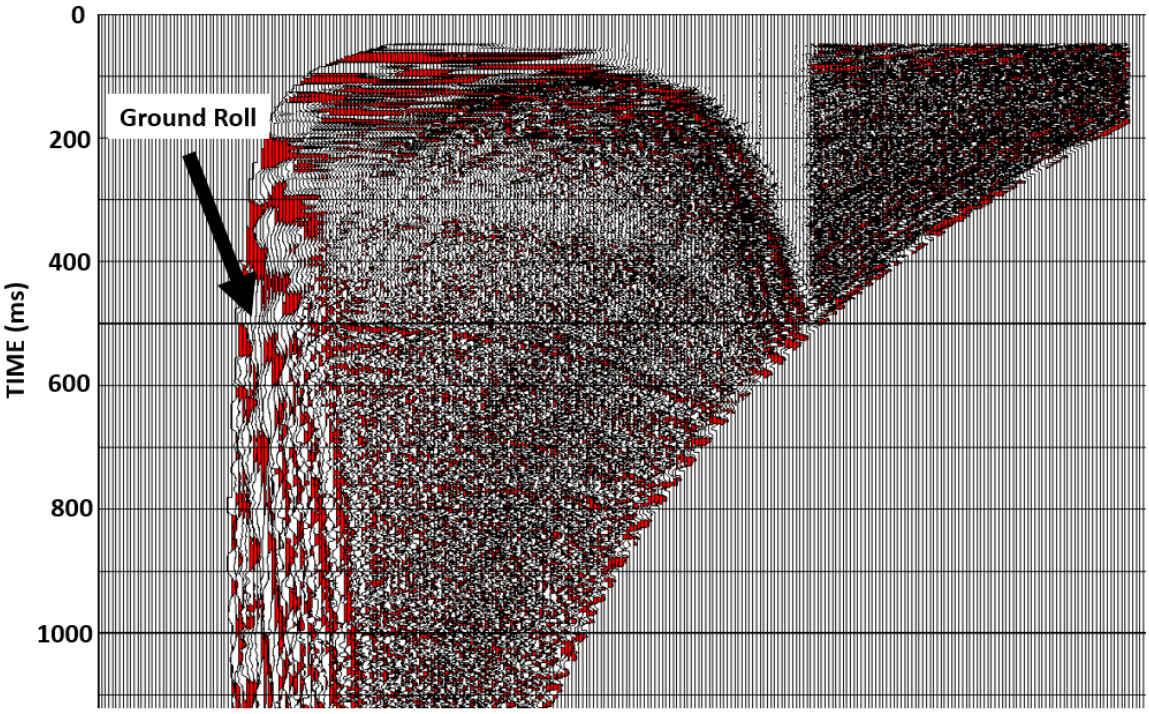

FIG 7. Radial transform of a shot gather.

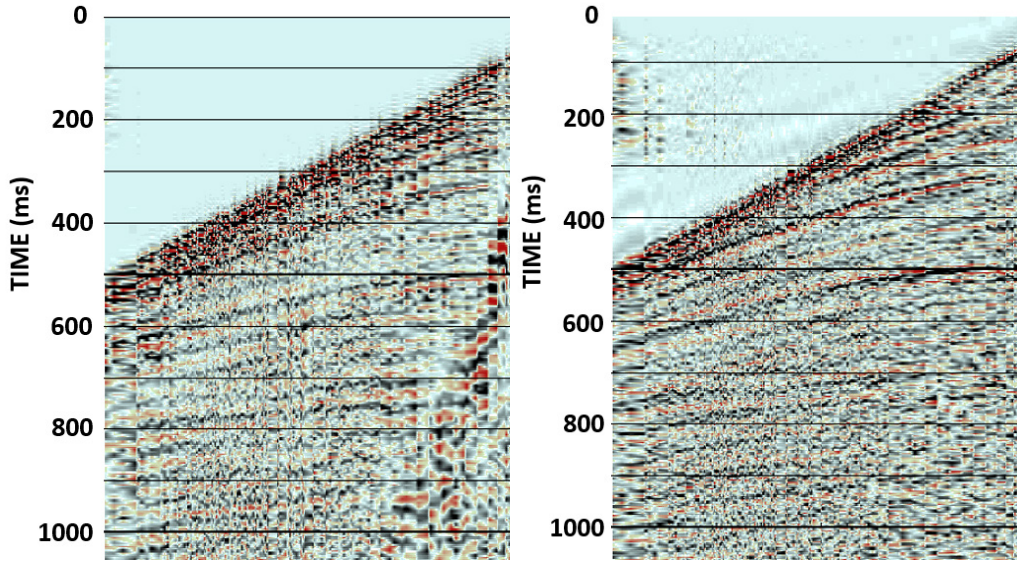

FIG. 8. Before (left) and after (right) Gabor deconvolution, after ground roll suppression

Three iterations of velocity analysis and residual statics were applied to correct for normal moveout and resolve any remaining statics errors in the seismic data. RMS velocity volumes were obtained by picking velocity profiles at certain common midpoint bin locations. Velocity profiles were picked based on hyperbolic semblance, common offset stacks and constant velocity stacks (Figure 9). This velocity analysis method is a robust

way to obtain RMS velocities from seismic data. Following velocity analysis and NMO correction, residual statics were calculated and applied using the stack-power maximization technique. This residual statics algorithm is surface-consistent. A pre-stack shot gather (Figure 10), shows clear, NMO corrected reflection horizons.

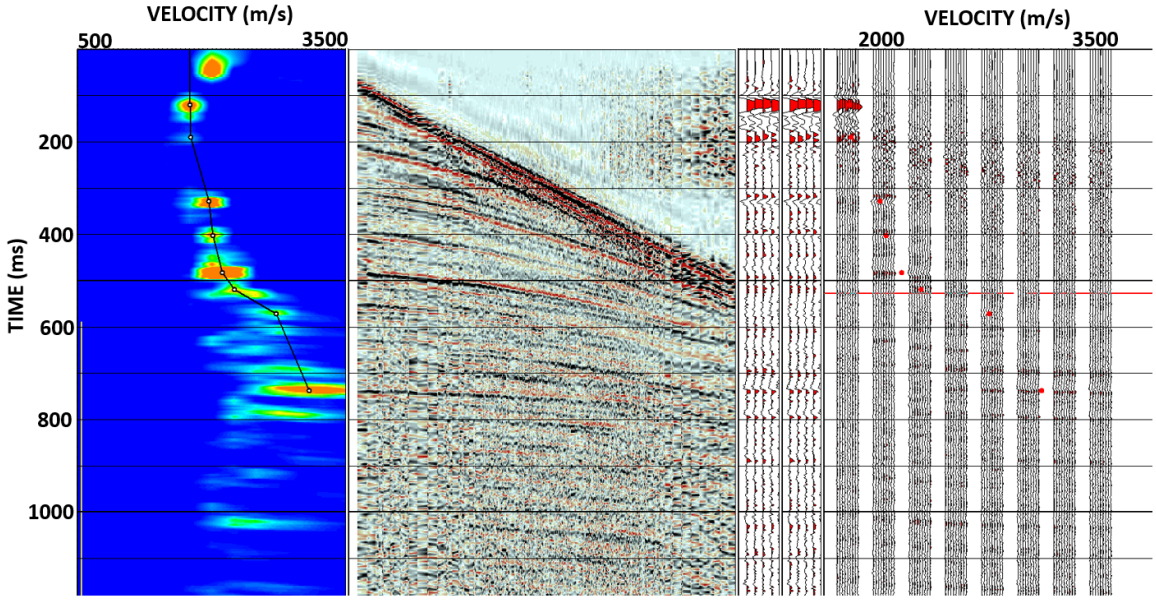

FIG. 9. Velocity analysis picking window.

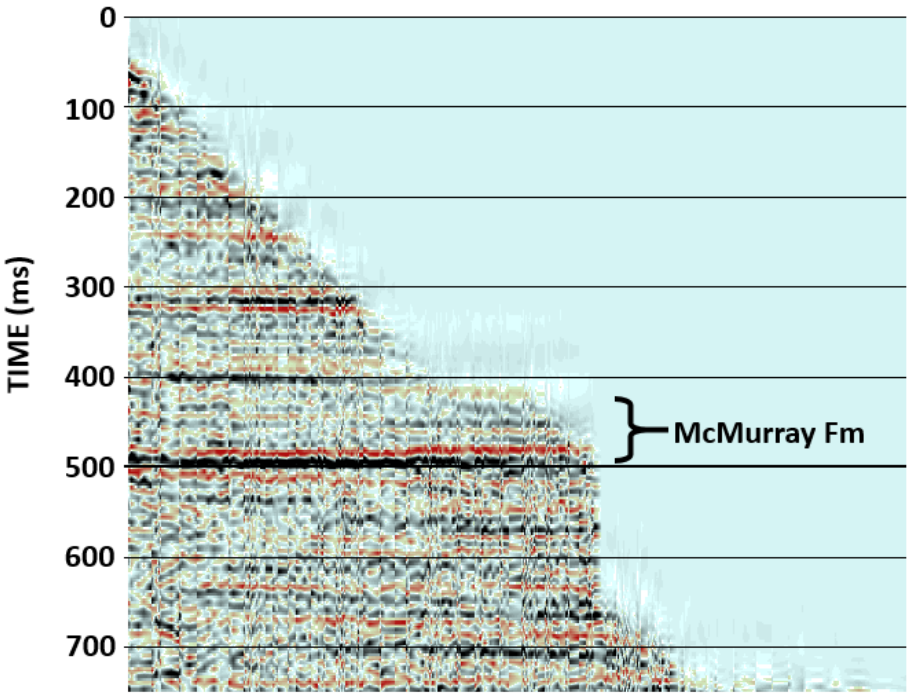

FIG. 10. Pre-stack shot gather example following 3 iterations of velocity analysis and residual statics, NMO mute applied.

Stacking is an effective tool to increase signal to noise ratio. Traces that share a common midpoint were summed to form a single trace. The traces that are summed will have variable azimuths and offsets. The number of traces summed at a given CMP is called the fold. Average fold in the survey is 28 and the maximum fold is 46; fold statistics are shown in Figure 11. Following the stacking process, phase-shift plus interpolation migration geometrically relocates seismic events to their proper position. The strata in the Athabasca region has relatively mild structure so migration is not an extreme process. Signal to noise was further enhanced through F-XY deconvolution which attenuates random noise. A migrated section is shown in Figure 12. The final PP stacked volume shows high signal to noise ratio and pervasive reflection horizons in the interval of interest, 250ms to 550 ms.

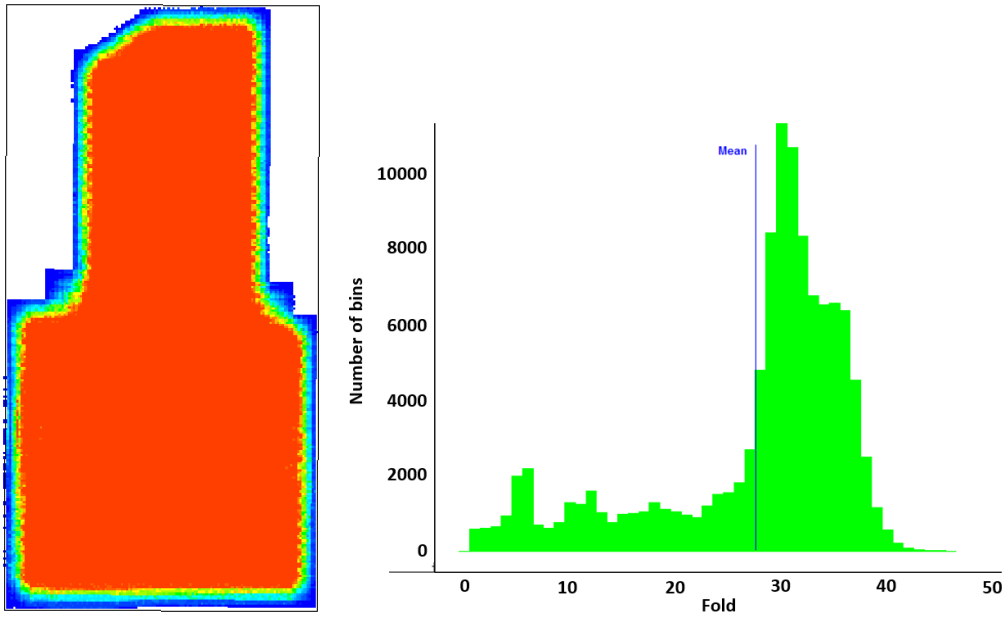

FIG. 11. PP seismic fold statistics.

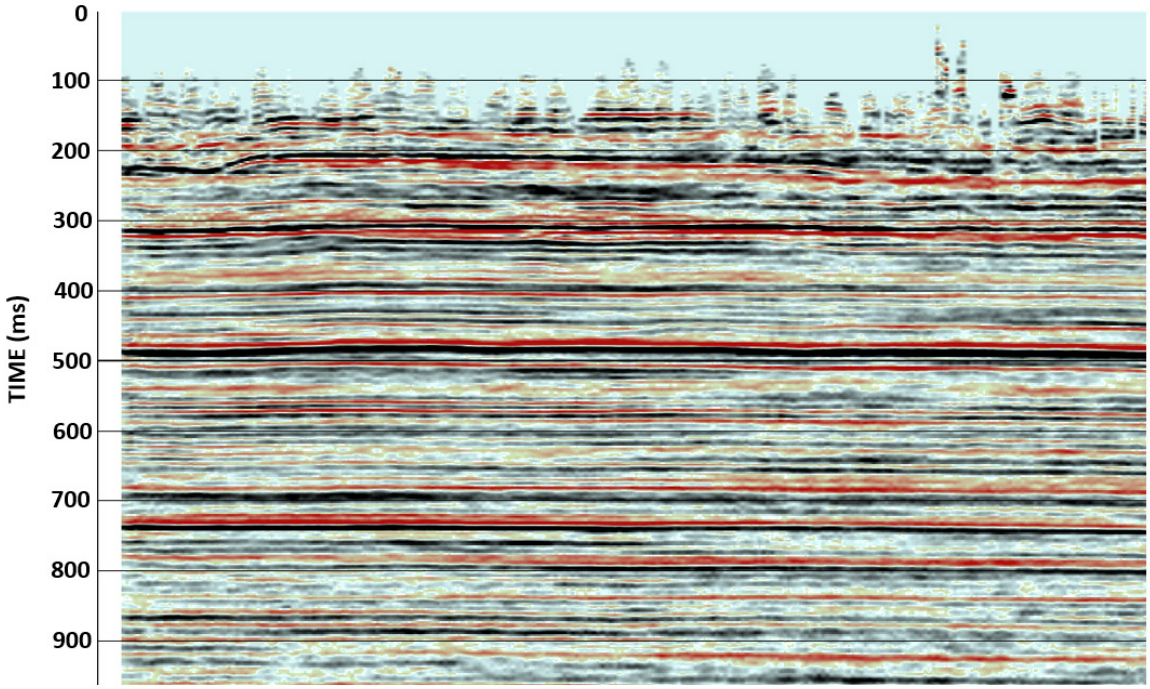

FIG. 12. Vertical component stacked, migrated seismic section example.

PS processing

Some of the outputs from the PP processing are necessary to effectively process the PS seismic data to an interpretable point. The incident raypath for a converted wave is a compressional. To process PS data, PP shot statics and PP RMS velocities are used initially. The processing flow for the PS seismic data is similar to the PP processing, with some key differences. Statics, velocity analysis and conversion point binning have differences from those performed for strictly compressional reflections.

The binning grid from the PP geometry assignment is common to the PS seismic data. The raw traces from the field exist as vertical, inline and crossline components, since the 3 component geophones are oriented with magnetic North. Inline and crossline geophone components were rotated into radial and transverse components. Converted wave reflections were limited to only radial shot gathers (Figures 4 and 5), implying horizontal isotropy. P wave shot statics and P and S wave elevation statics are applied next. P wave shot statics are taken from the PP processing. Radial transform denoise, Gabor deconvolution and spectral balancing were all applied in a similar fashion to the vertical component processing.

Converted wave velocity analysis uses a similar methodology to PP velocity analysis. The output of converted wave velocity analysis are converted wave stacking velocities, which can be used to correct normal moveout for converted wave reflections. Immediately after correcting for PS NMO, common receiver stacks were generated. Common receiver stacks were used to estimate shear statics. The overburden usually has low, complex and variable shear wave velocities which can have large static effects on converted wave reflections. Estimating receiver statics from common offset stacks has three main steps:

horizon picking, horizon smoothing and horizon subtraction. Regionally extensive horizons were first picked on the common receiver stacks. These picked horizons are smoothed to obtain a regional trend. The static value is acquired by subtracting the original horizon pick from the smoothed horizon. It is important to pick several different events and calculate several different receiver statics to avoid biasing the static corrections to regional structure of a single reflection. Figure 13 depicts a radial component receiver stack with a picked horizon and Figure 14 shows a radial component receiver stack with the application of receiver statics.

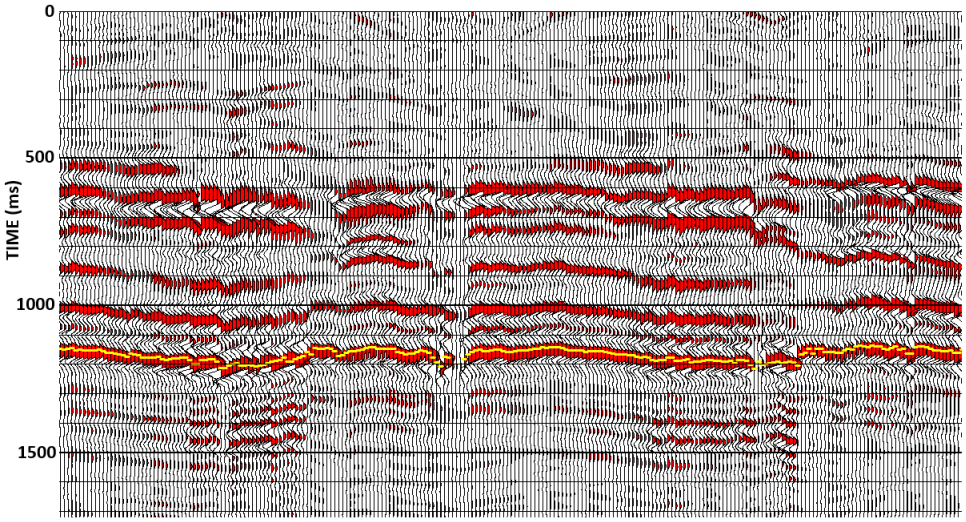

FIG. 13. Radial component common receiver stack with a picked horizon.

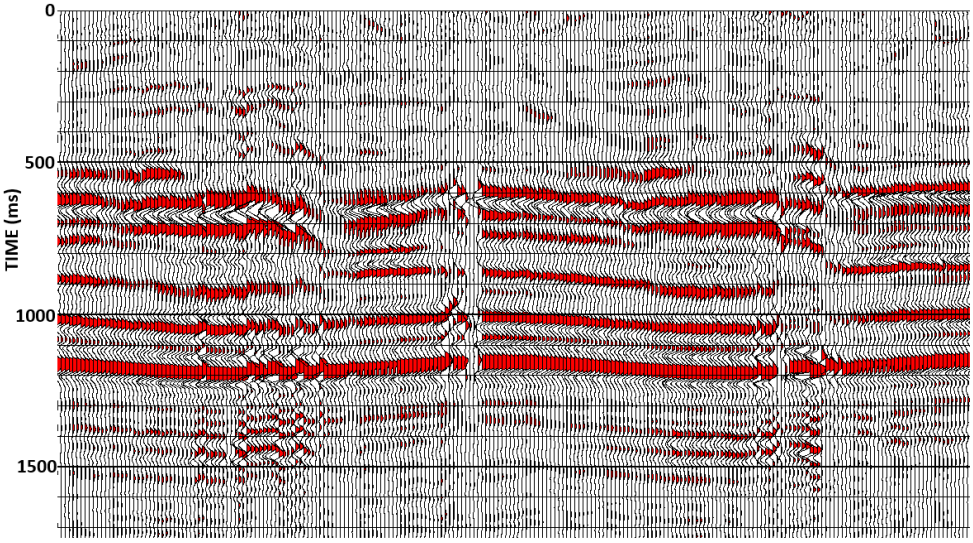

FIG. 14. Radial component common receiver stack after application of a horizon-based receiver static.

Converted wave reflections exhibit asymmetry in their raypaths (Figure 15). Conventional CMP stacking cannot properly place converted wave conversion points. The point in which a converted wave reflects is variable with depth. Close to the surface, the conversion point is near the receiver and moves away with depth. As depth increases, the conversion point approaches an asymptote. A simple way to stack converted wave reflection data is to initially use an asymptotic common conversion point. Using a constant V_p/V_s, preferably from the main interval of interest, data is stacked for the asymptotic conversion point. This method is effective in stacking deeper converted wave reflections, and uncertainty increases towards the surface. A variable V_p/V_s can be generated from PP and PS stacking velocities which can then be used to calculate the true conversion points of PS reflections. Figures 16 and 17 display an asymptotic common conversion point stack and a common conversion point stack respectively. At depths below 400 ms the differences are negligible. However, there are slight differences in the near surface. The shallow events are more coherent on the common conversion point stack, which is expected due to the differences in the stacking procedures.

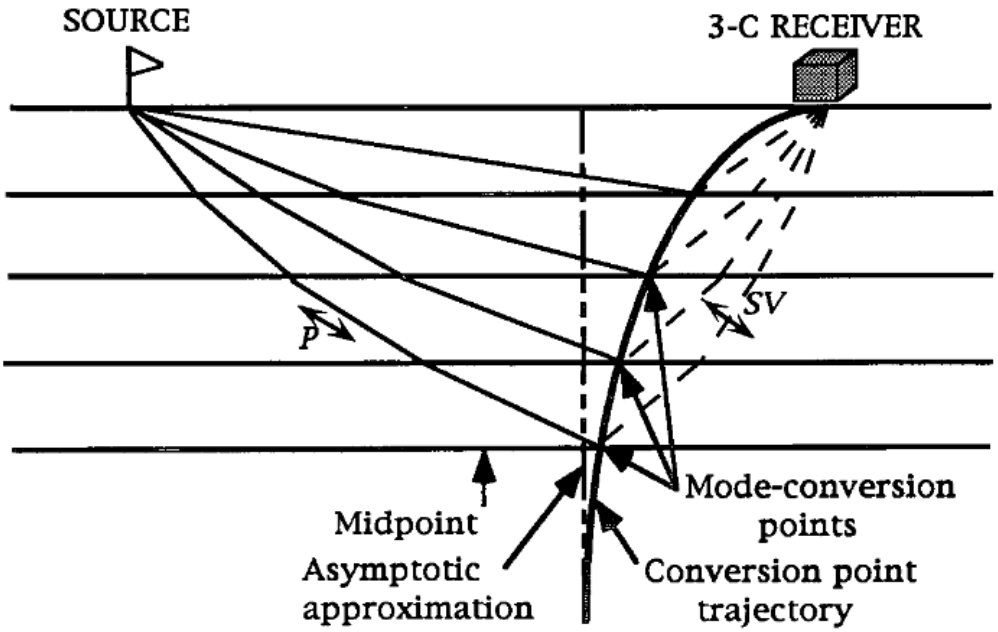

FIG. 15. Reflection raypath geometry for a converted wave. The midpoint, conversion point and the asymptote of the conversion point are shown (Schafer, 1992).

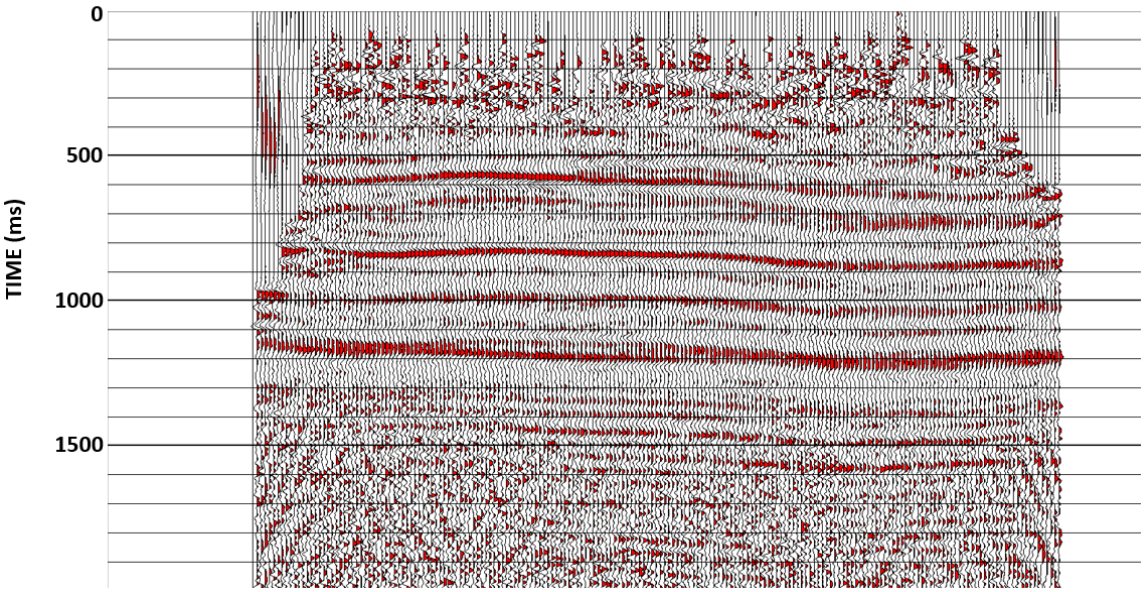

FIG. 16. Radial component asymptotic common conversion point stack

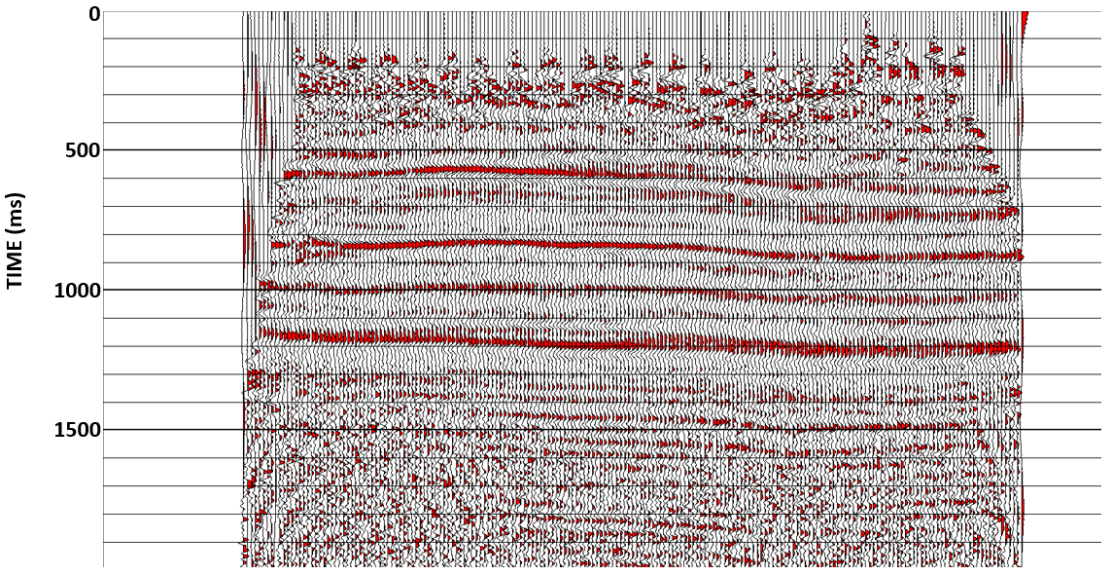

FIG.17. Radial component common conversion point stack

Figure 18 shows data examples for the fully processed PP and PS stacked seismic data. Both volumes display reflection horizons that span across the survey. The PP seismic data contains much higher frequencies than the PS seismic data. Both volumes have fairly good signal to noise ratio.

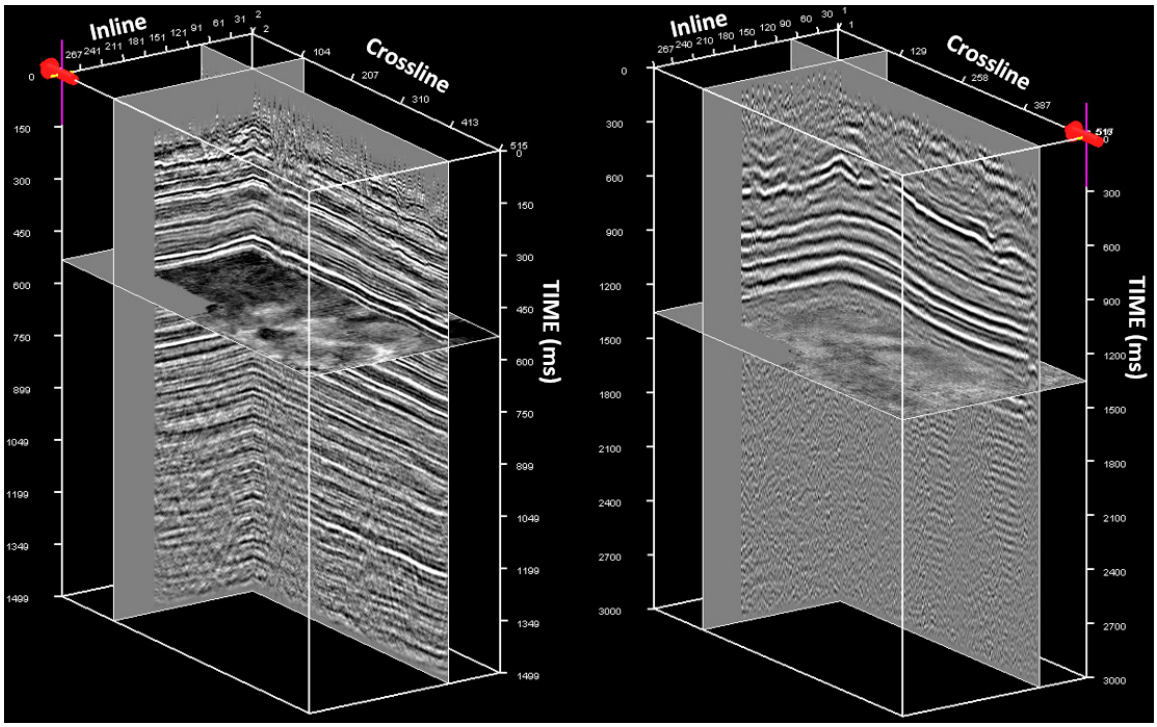

FIG. 18. 3D visualization of fully processed PP seismic data (left) and PS seismic data (right).

INTERPRETATION AND ANALYSIS

The interpretation workflow for the study starts at a large, regional scale and detail is added progressively. The tools utilized to delineate geology from the seismic data were similar for both the PP and PS datasets. The PP seismic data was interpreted first, due to the higher signal to noise ratio, higher frequency content and availability of compressional sonic logs. The study area has a relatively high well density, and the geology is well understood.

PP and PS regional interpretation

A synthetic seismogram tying the well log data to the PP seismic data is shown in Figure 19. The input to the synthetic seismogram were despiked density and sonic logs and a statistically extracted wavelet from the seismic data within the interval of interest. Cross-correlating the synthetic seismogram with the true data traces yields a maximum value of 0.65, indicating a relatively close match. Known positions of geological interfaces were taken from the well log information, and applied to the seismic reflection data after correlation. PP seismic stratigraphic interpretation is annotated in Figure 21, and the same section free of annotations is shown in Figure 20. Reflection continuity is very good for the Paleozoic unconformity, Clearwater Formation and Grand Rapids Formation. However, the McMurray Formation and Colorado-Quaternary Unconformity have poorer reflection continuity. For each of the main stratigraphic units, time structure surfaces were made. Time structure is a useful metric for understand geology in the Athabasca Oil Sands. Isochron maps were made for the key intervals.

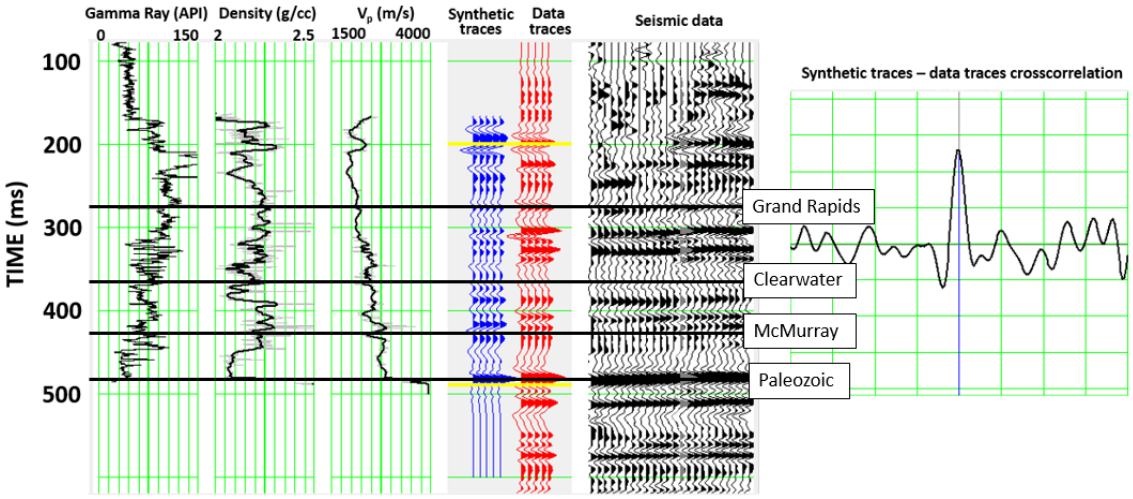

FIG. 19. Synthetic seismogram for stacked PP seismic data. Blue traces represent the synthetic seismogram, red traces represent data traces at the well location. Maximum cross correlation 0.650.

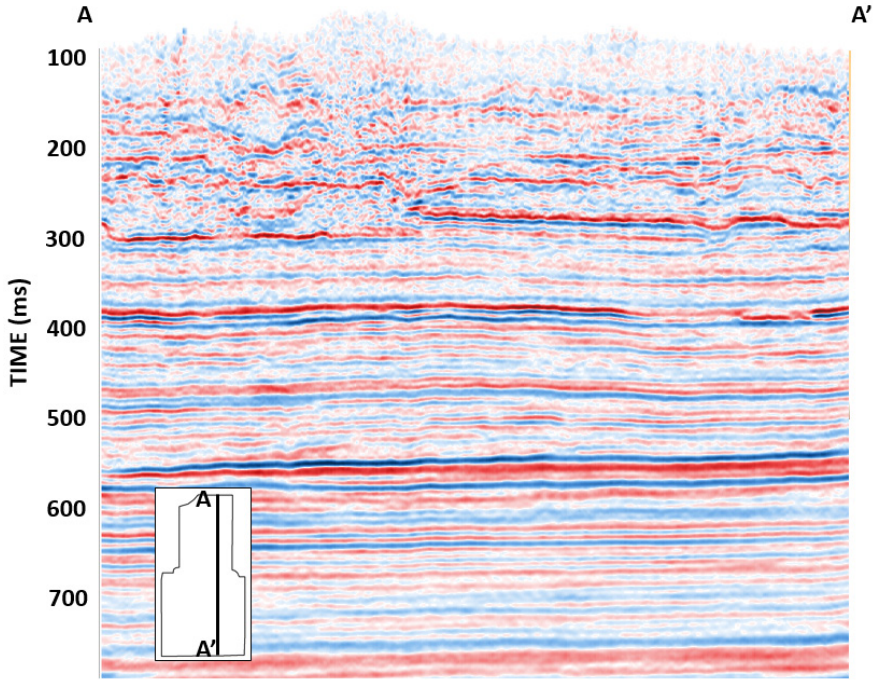

FIG. 20. Example PP seismic section uninterpreted.

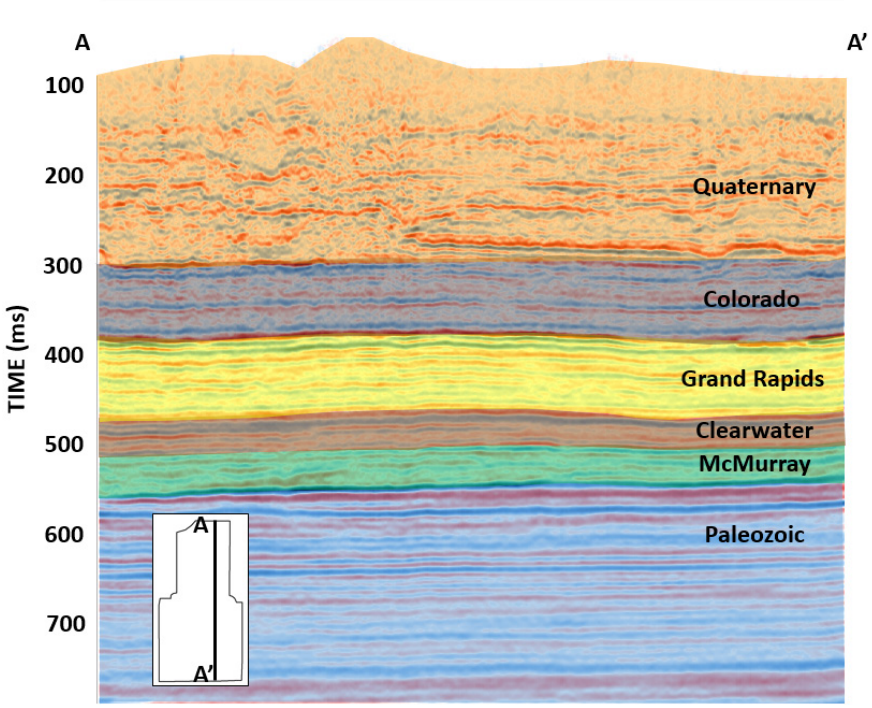

FIG. 21. Example PP seismic stratigraphy interpreted

After interpreting the P wave data, the converted wave reflections can be more easily analyzed. Converted wave synthetic seismograms, which are more complex than PP synthetic seismograms, were made to compare well log data to seismic data traces. A converted wave synthetic seismogram is shown in Figure 22. The converted wave synthetic seismogram and the converted wave data traces have a maximum crosscorrelation of 0.600, indicating a fairly good synthetic tie. In similar fashion to the PP dataset, seismic stratigraphy can be defined after tying the surface seismic data to the well log data. An uninterpreted PS seismic section is shown in figure 23 and a PS seismic section with stratigraphic interpretation is shown in Figure 24. The horizons on the PS data are, for the most part, more pervasive than on the PP seismic data. The McMurray Fm is a very marginal pick on the PP seismic data, but on the PS volume, it is a fairly pervasive horizon. This fact already shows that collecting and processing PS data is a viable tool in an oil and gas exploration scenario. With the picking of pervasive reflection horizons, time structure surfaces were output. Isochron maps were also made for intervals of interest.

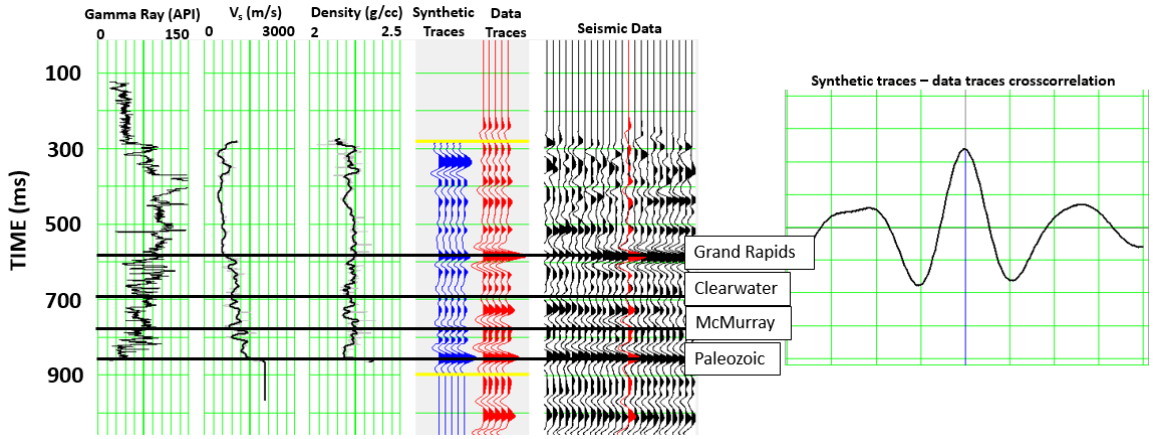

FIG. 22. Synthetic seismogram for stacked PS seismic data. Blue traces represent the synthetic seismogram, red traces represent data traces at the well location. Maximum cross correlation 0.600.

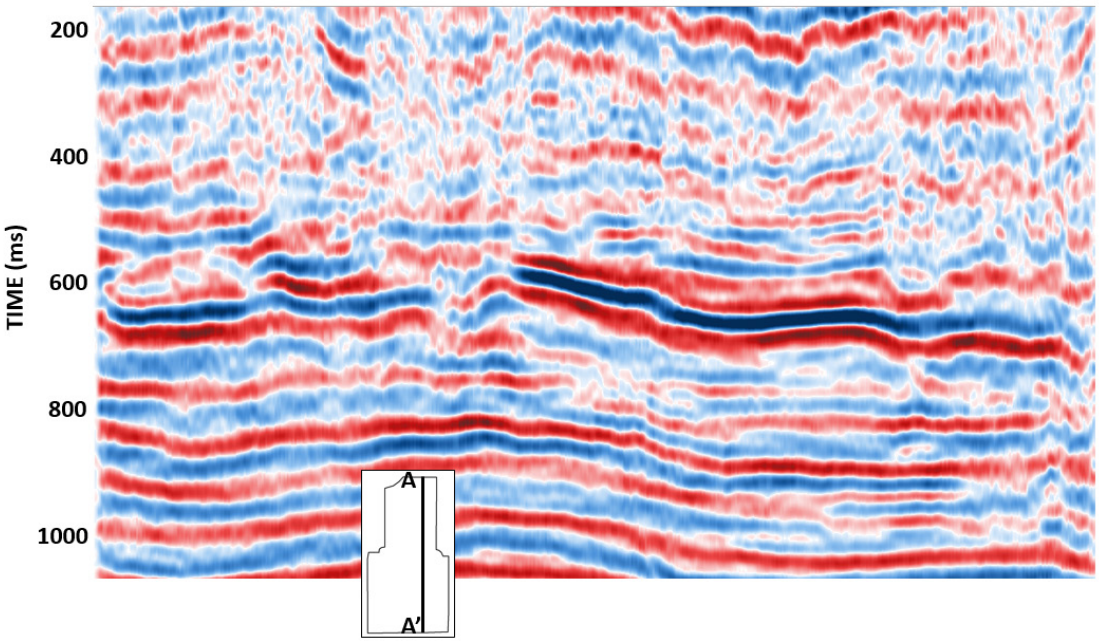

FIG. 23. Example PS seismic section uninterpreted.

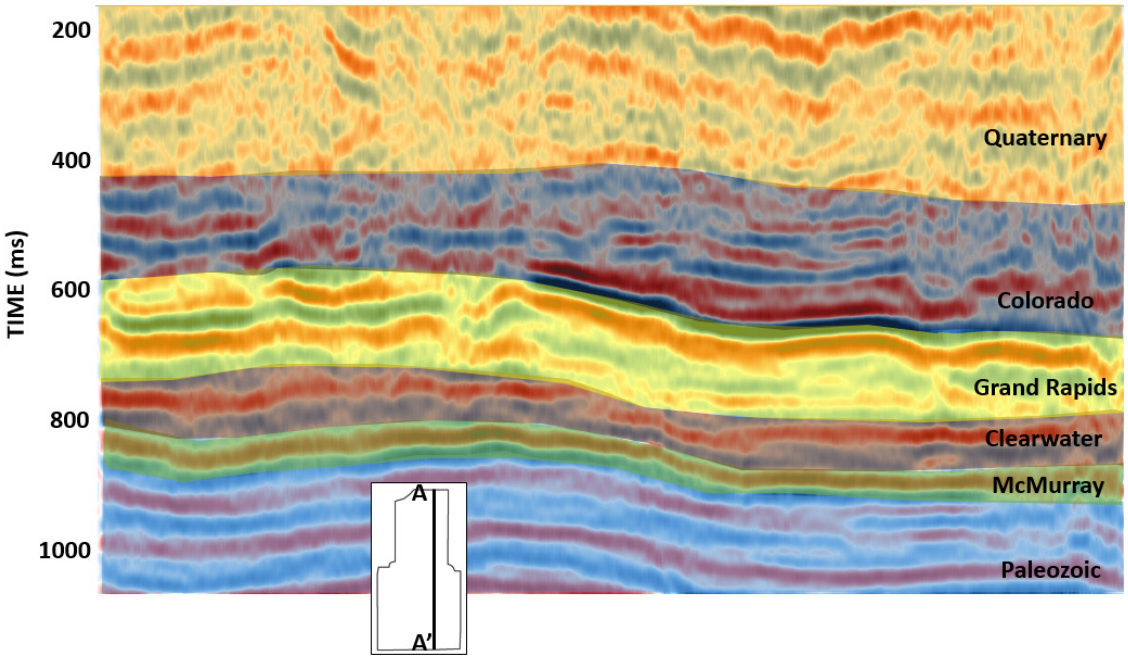

FIG. 24. Example PS seismic interpreted.

In addition to basic stacked synthetic seismograms, offset synthetic seismograms were generated using the CREWES Syngram system. These offset synthetics act as a secondary correlation tool with surface seismic and also a tool to model amplitude versus offset response. An offset PP synthetic seismogram is shown in Figure 25 and an offset PS synthetic is shown in Figure 26. Both offset synthetic seismograms have a maximum offset to depth ratio of 1 beyond which data are truncated. This data truncation mimics the effect of an NMO mute. There are some AVO effects in both synthetics; the PS synthetic has much more AVO than the PP synthetic. The increased AVO magnitude in the PS synthetic is expected, mode conversion only occurs at non-normal incidence.

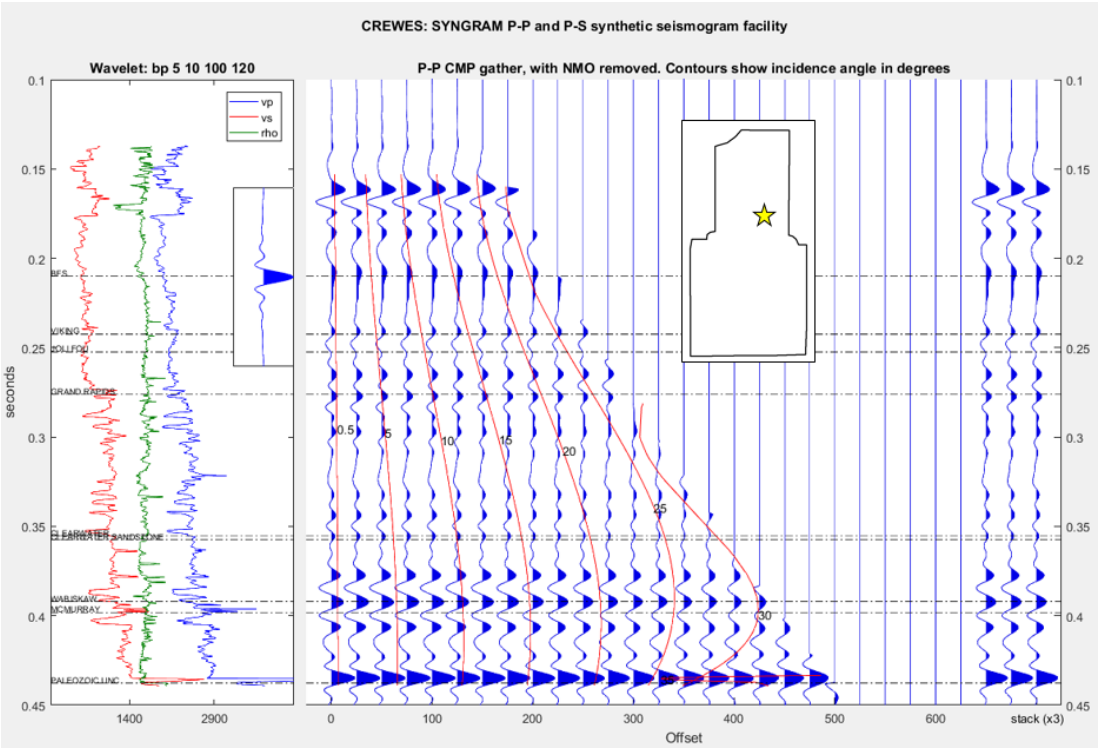

FIG. 25. Variable offset synthetic seismogram, PP response.

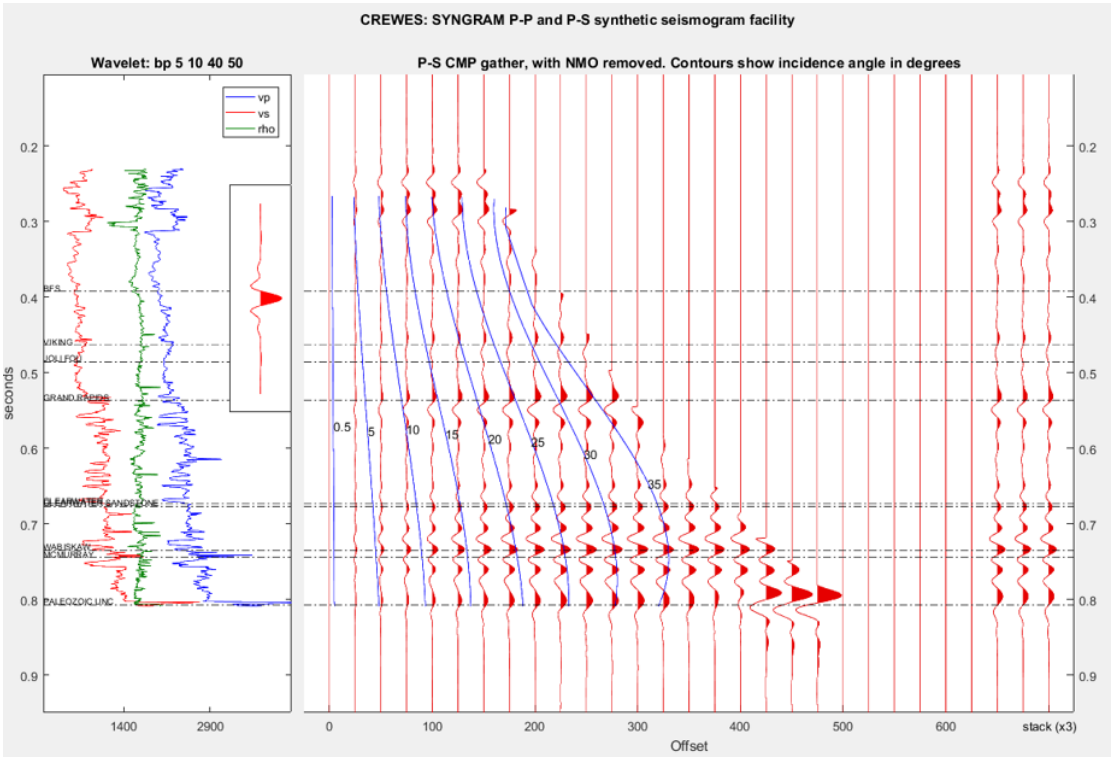

FIG. 26. Variable offset synthetic seismogram, PS response.

The bitumen saturation in the Upper McMurray Formation is strongly dependent on lithology. Therefore, when exploring for hydrocarbon targets in the McMurray, one must find stratigraphically thick, porous, "clean" sands. The diagenetic processes that act on sandy sediments are different than those of shaly sediments. As the deposits are compacted, the volume taken up by shales will decrease much more than for sands. This effect is called differential compaction. A few seismic tools when used in conjunction are effective at studying the extent of differential compaction in the McMurray formation. Time structure can highlight structural highs in the McMurray. These structural highs may indicate sand concentrations when there are adjacent shales. Isochron maps can show the thicknesses of the McMurray Formation and also indicate better quality reservoir. Ideally, high time structure and thick isochron should indicate the best reservoir when considering strictly differential compaction.

Paleozoic and McMurray PP time structure are shown in Figure 27 and the McMurray to Paleozoic PP isochron is shown in Figure 28. The McMurray and Paleozoic time structure show similar long wavelength trends. There are structural lows in the northern and southwest parts of the survey area. The structure of the McMurray is heavily influenced by the topography of the pre-Cretaceous unconformity. The isochron map (Figure 28) does however highlight some of the structural differences between the two surfaces. The isochron map shows a thick package of sediment trending from the northeast to the southwest. The thick sediment package lies coincident with a structurally high McMurray trend. By differential compaction, these properties may indicate a sand concentration in the McMurray. From the known regional geology, a McMurray B aged valley-fill is expected to be present in the project area. A flattened seismic cross section reveals a truncation of the regional McMurray seismic character in the region of high McMurray structure and thick McMurray-Paleozoic isochron (Figure 29). An existing well drilled into the McMurray B aged channel, shows a non-regional facies (Figure 30). These non-regional facies appear to be mostly inclined heterolithic strata (IHS) made of predominantly mudstones and to a lesser extent sandstones. These muddy IHS facies are marginal reservoir at best, however other parts of large McMurray channel systems are very prospective for oil sands thermal extraction. A converted wave cross section through the McMurray channel shows a seismic character change in the McMurray channel (Figure 31). The obvious truncations of regional McMurray seen on the PP seismic data are not present on the converted wave seismic data. However, the McMurray top reflection on the converted wave seismic data is much more regionally coherent than on the PP dataset. An interval RMS amplitude map of the Upper McMurray on the converted wave seismic data is shown in Figure 32. The approximate position of the McMurray B2 aged channel feature is highlighted on Figure 32. There is high variability in converted wave amplitude within the McMurray channel. The amplitudes may vary with the quality of the reservoir.

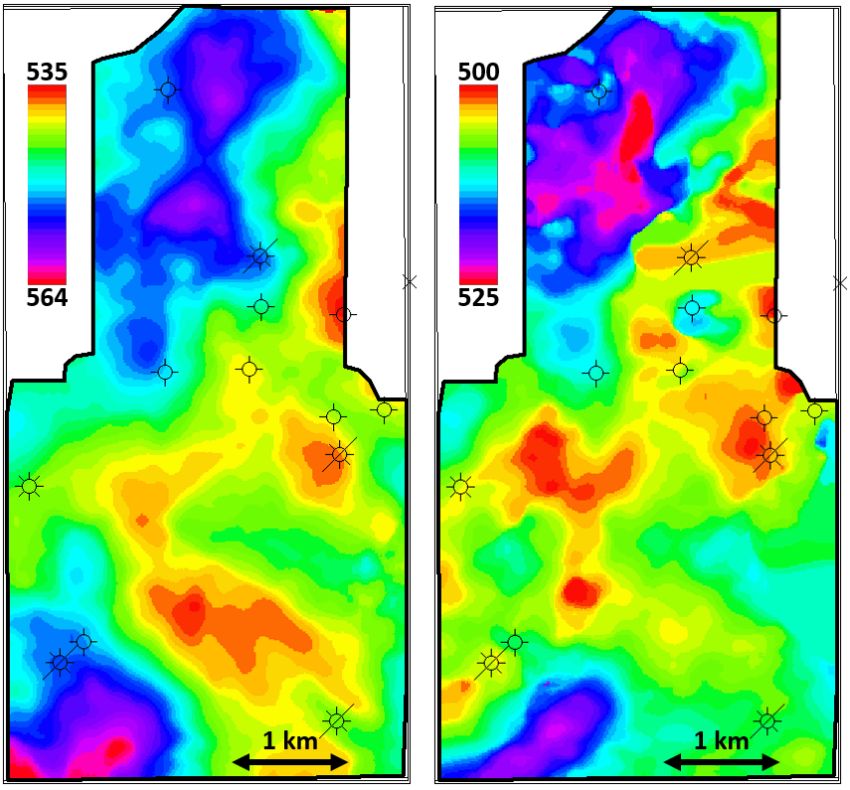

FIG. 27. Paleozoic (left) and McMurray (right) PP time structure in milliseconds.

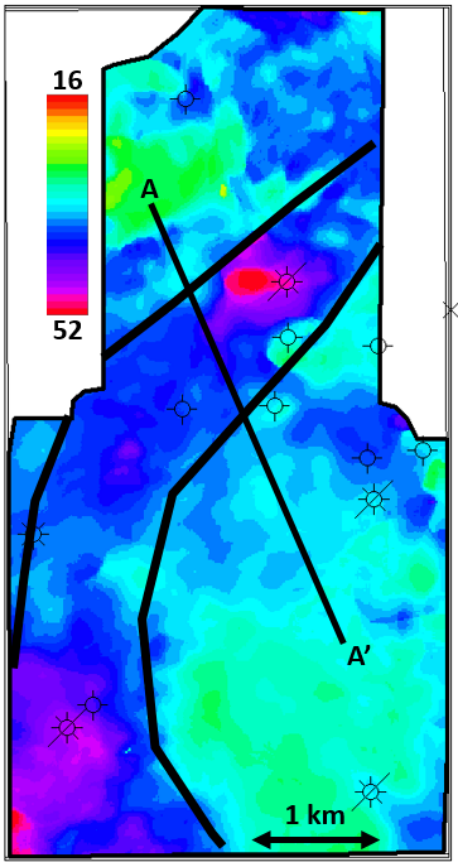

FIG. 28. McMurray – Paleozoic isochron in milliseconds.

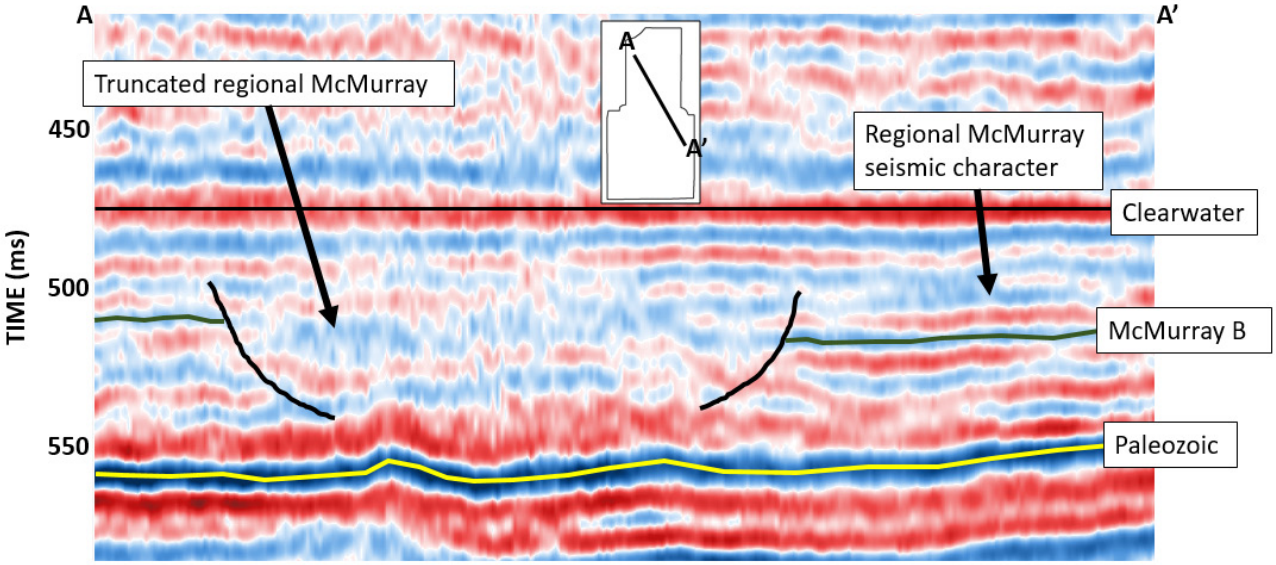

FIG. 29 Cross section through high structure, thick isochron of the McMurray Fm. Regional McMurray seismic character is truncated, against the channel.

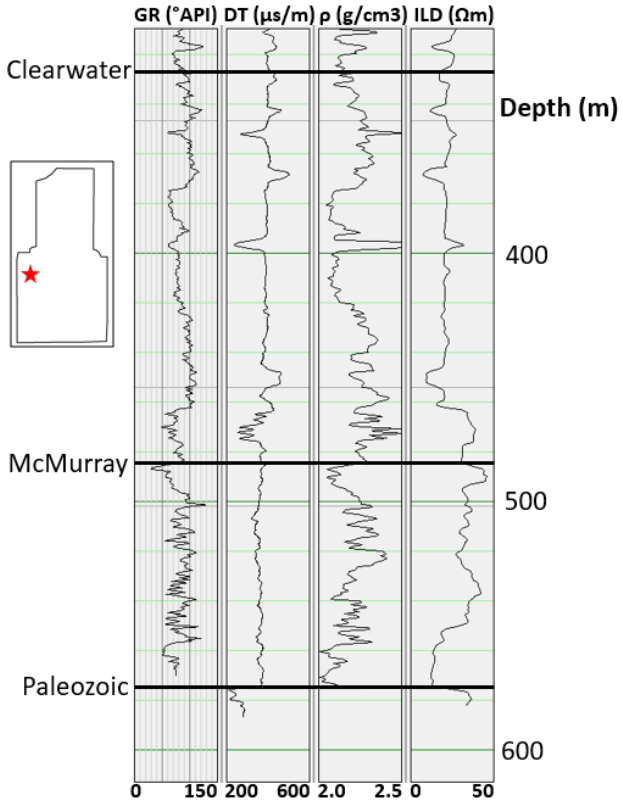

FIG. 30. Well log through seismically located McMurray channel.

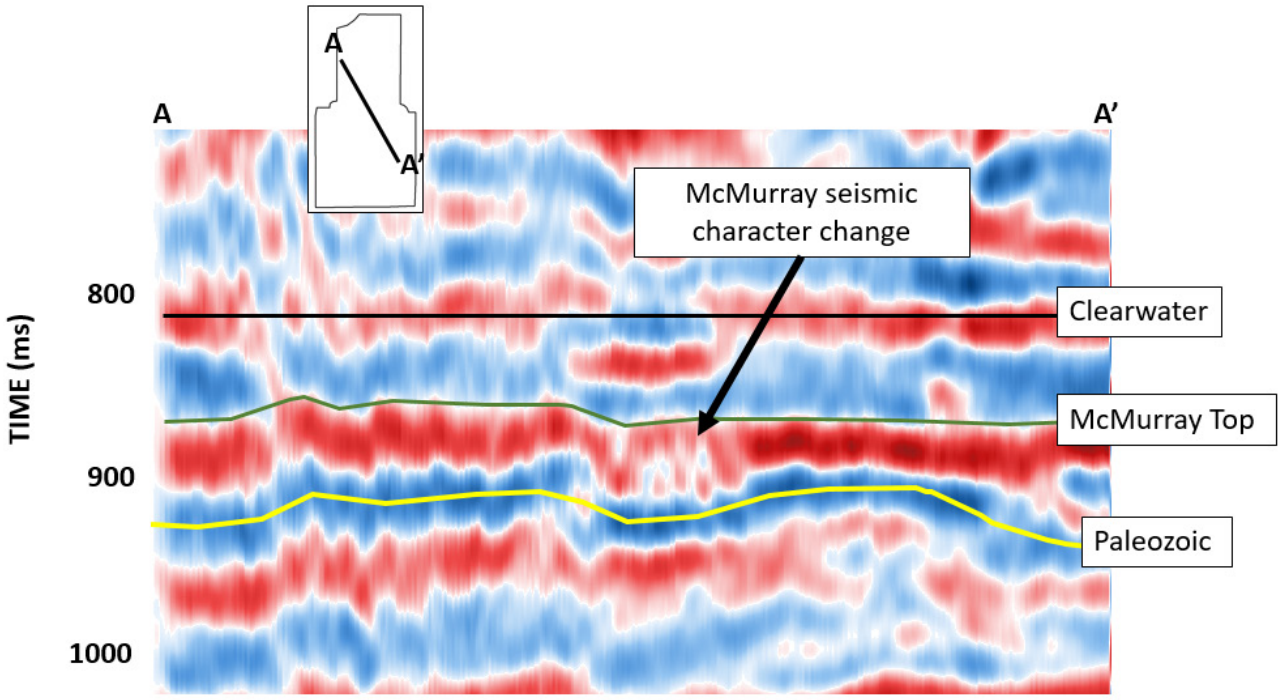

FIG. 31. PS cross section through McMurray channel.

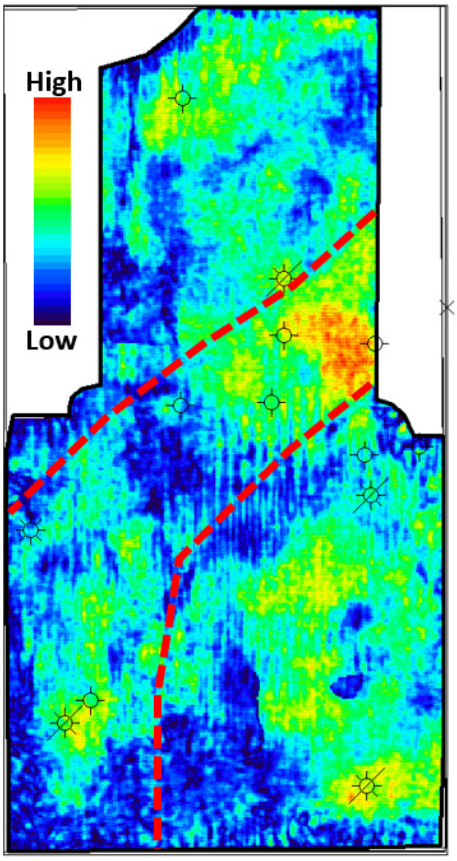

FIG. 32. Converted wave interval RMS amplitude for Upper McMurray. Approximate position of McMurray B2 channel highlighted.

An effective tool to understand in-situ fluid properties in the McMurray Formation is interval amplitude maps. If the root mean square (RMS) amplitude is taken in a given window, the resultant map may reveal the distribution of natural gas in this window. Figure 33 shows the natural gas presence in the Upper McMurray based on RMS amplitude. These findings correlate to wells (Figure 34).

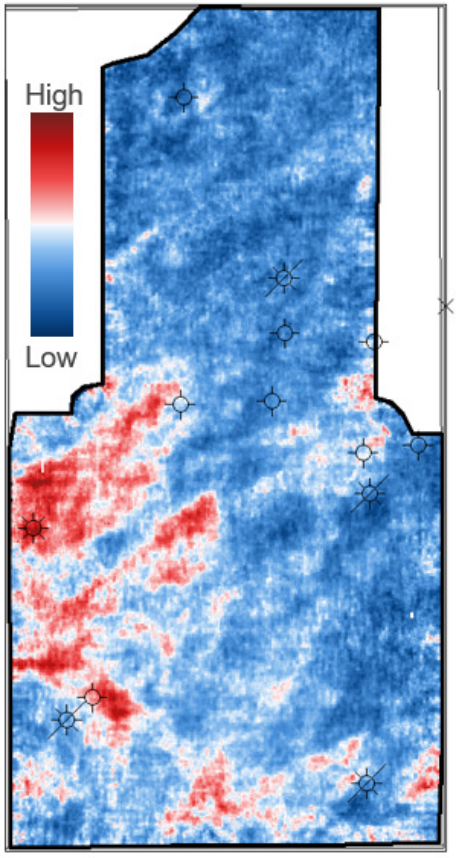

FIG. 33. PP RMS amplitude for the Upper McMurray. In-situ natural gas is red.

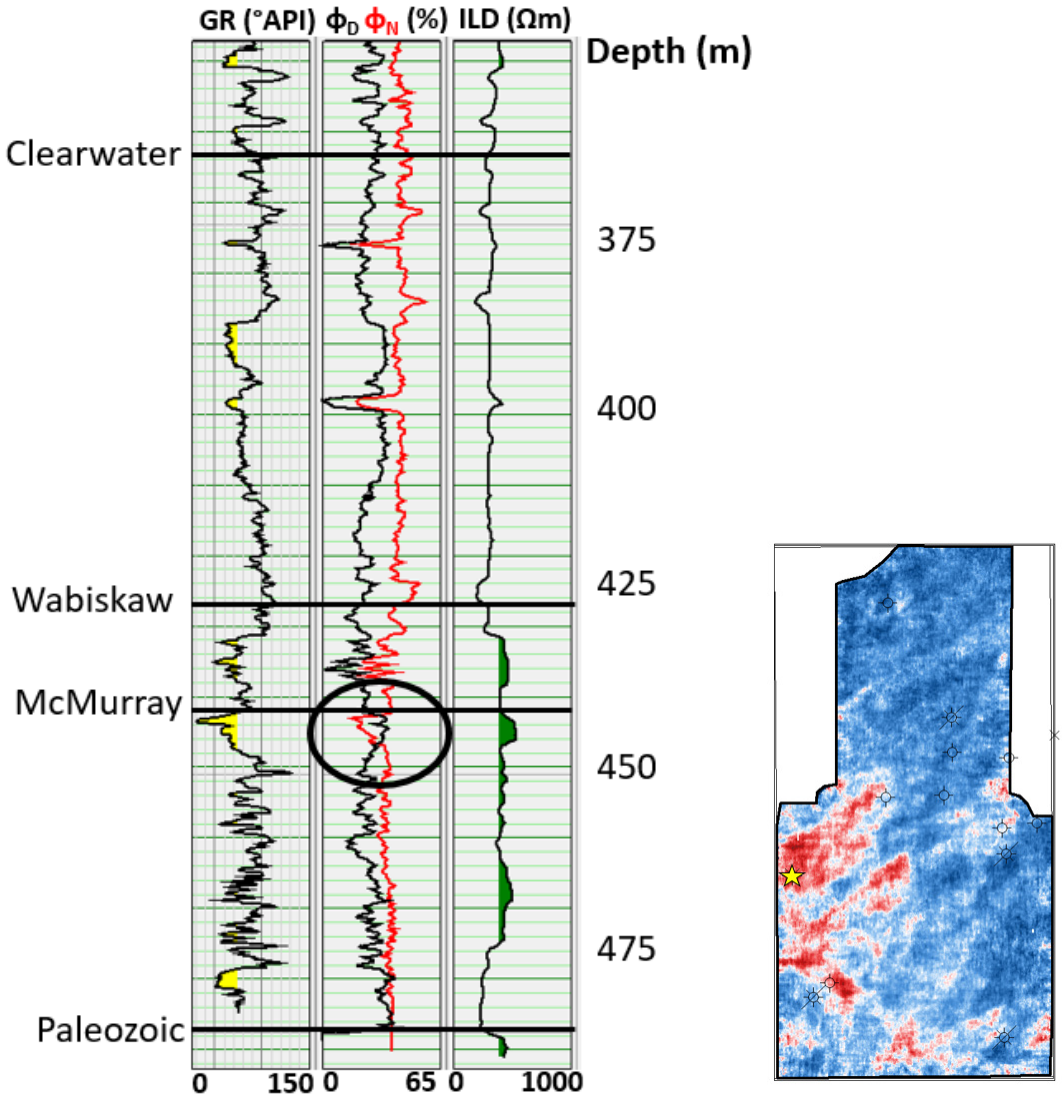

FIG. 34. Well log through region with seismically detected gas. Gas presence is confirmed by density porosity and neutron porosity log crossover, which is circled in black.

The Colorado group is seismically much more quiescent compared to the McMurray formation, with the exception of the Colorado-Quaternary interface. The majority of Colorado group time slices show no significant local anomalies, consistent with the marine shale lithology (Figure 35). However the Upper Colorado (Figure 35) shows erosional features cutting down from the above Quaternary. Time structure maps from the top Colorado Group are relatively difficult to produce for the PP seismic data due to the inconsistency of the reflection pick. However, a time structure map with fairly high uncertainty was created, and is shown in Figure 36. The Top Colorado Group time structure map shows an anomaly in the vicinity of the Quaternary channel feature interpreted from Figure 35. It is valuable to know exactly where the Quaternary fluvial systems are for a number of reasons, most notably, drilling risk. The channels have very different geology from the surrounding marine shales of the Colorado. Also, the Quaternary channels have very different seismic properties from the surrounding rock, which can affect processing.

It is important to choose velocity analysis bins within the Quaternary channels to correctly process seismic data.

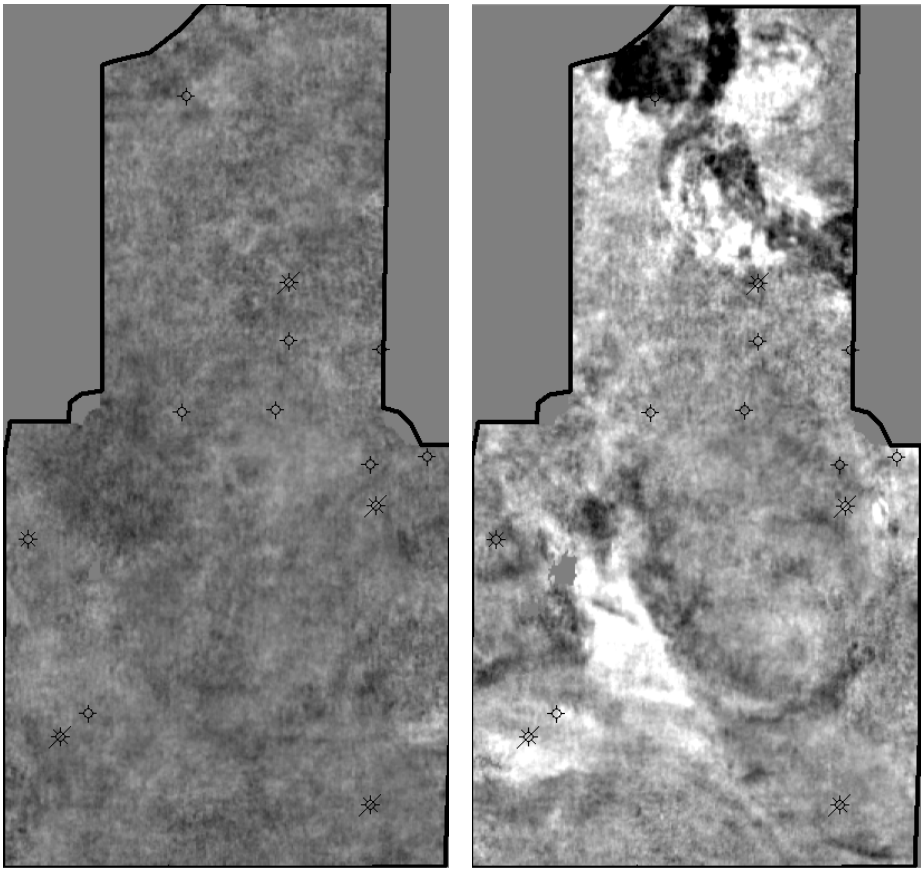

FIG. 35. Middle Colorado (left) and Upper Colorado (right) amplitude time slices.

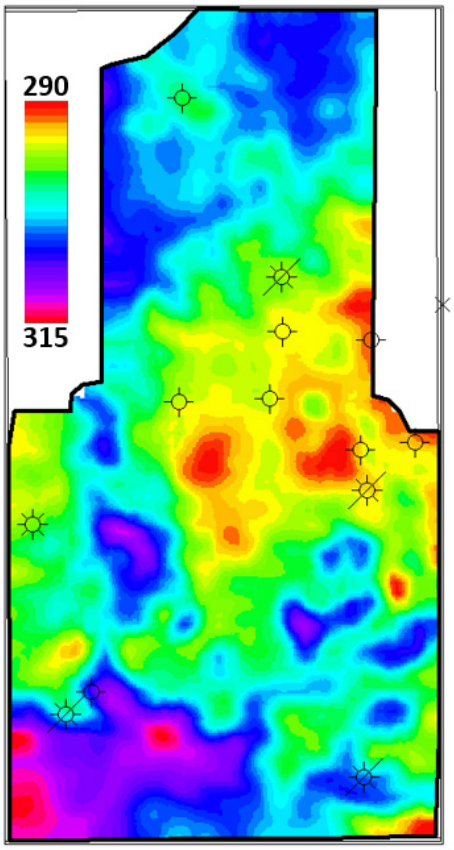

FIG. 36. Quaternary – Colorado interface time structure in milliseconds for PP seismic data.

Using only isochron maps for the PP and PS seismic volumes, interval V_p/V_s values can be found. The equation for interval V_p/V_s is given in equation 1. The variables, Δt_{pp} and Δt_{ps}, are defined as PP and PS isochron respectively. Interval V_p/V_s is an effective way to obtain a physical rock parameter without inversion. Picking uncertainty has a very large effect on interval V_p/V_s so it is very important to use large intervals to reduce this error (Figure #). For example, when creating an interval V_p/V_s map for the McMurray-Paleozoic interval large anomalies could stem from improper horizon picks. In Figure 37, very high V_p/V_s zones are a result of bad picks instead of from geology. To generate a better map, a larger interval should be used. Figure 38 shows the interval V_p/V_s map for the Grand Rapids to Paleozoic interval. This is a much larger interval and the V_p/V_s map is much less sensitive to minor picking errors. However, edge effects are still present. An erroneous V_p/V_s value of 1 exists in the northwest corner of the Grand Rapids - Paleozoic V_p/V_s map (Figure 39). Unfortunately, due to the large intervals that must be used to obtain adequate interval V_p/V_s maps, it is challenging to make detailed reservoir interpretations. Thus, interpretation of interval V_p/V_s maps is limited to large scale, regional interpretations, which are still valuable. Horizon based interval V_p/V_s can also be used to quality control inversion results. Comparing horizon based interval V_p/V_s maps to inversion based RMS or interval average maps and correlating back to geological control can give a sense of the accuracy of the results.

$$\frac{V_p}{V_s} = 2\frac{\Delta t_{ps}}{\Delta t_{pp}} - 1 \quad (1)$$

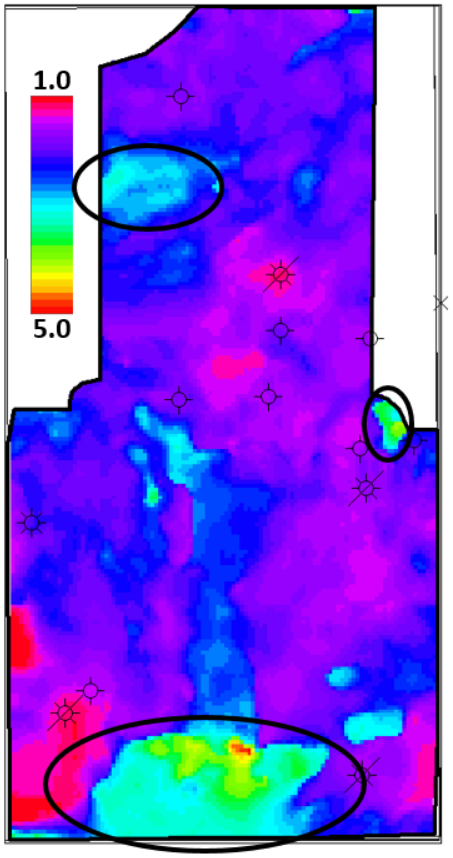

FIG. 37. McMurray – Paleozoic horizon based interval V_p/V_s. Anomalies highlighted with black circles represent areas with poor PP or PS horizon picks.

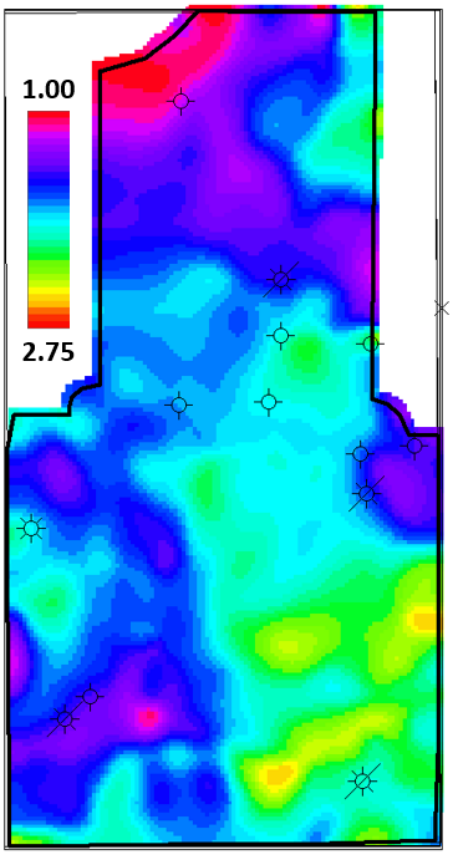

FIG. 38. Horizon based interval V_p/V_s for Grand Rapids – Paleozoic.

PP and PS inversion and rock physics

Several inversion methodologies were used in attempt to recover rock properties from the seismic volumes. The first technique used was model-based post-stack PP impedance inversion. A single inversion wavelet, obtained statistically from the post-stack PP seismic data in the interval of interest was used. A low frequency model (Figure 39) was generated using a smoothed regional interpretation and a single well log from the project area. The three most regionally pervasive reflection horizons, Grand Rapids Fm, Clearwater Fm and Paleozoic Unconformity, were used in the low frequency model creation. A high pass of 10 Hz and a high cut of 15 Hz was applied to the model. The generalized linear inversion (GLI) algorithm was used to obtain the inversion result. Small changes are added to the input low frequency model iteratively and synthetic traces are forward modelled from the updated model. The objective in the GLI algorithm is to minimize the error between the synthetic modelled data and the real seismic data. An inverted cross section is shown in Figure 40. Comparing inversion results to blind well logs, that is, well logs not involved in model generation, is an effective quality control method (Figure 40). The maximum crosscorrelation between the blind well log and the impedance volume is 0.85 in the interval of interest, indicating a good quality inversion result.

Similar to the use of interval RMS amplitude maps to detect the presence of natural gas, interval RMS impedance maps are effective in lithology detection. Upper McMurray RMS impedance (Figure 41) shows a high RMS impedance trend in approximately the same position as the McMurray B channel fill. Using the well logs in Figure 34 and 42, a correlation between high RMS impedance and better quality reservoir is inferred. In an exploration scenario, a drilling target would ideally have high RMS impedance in the McMurray Fm. Viewing a cross section of an impedance volume can also highlight zones with good reservoir. An impedance cross section, flattened on the Clearwater Fm, through the McMurray B2 channel trend with the thickest isochron reveals zones with highest impedance (Figure 43).

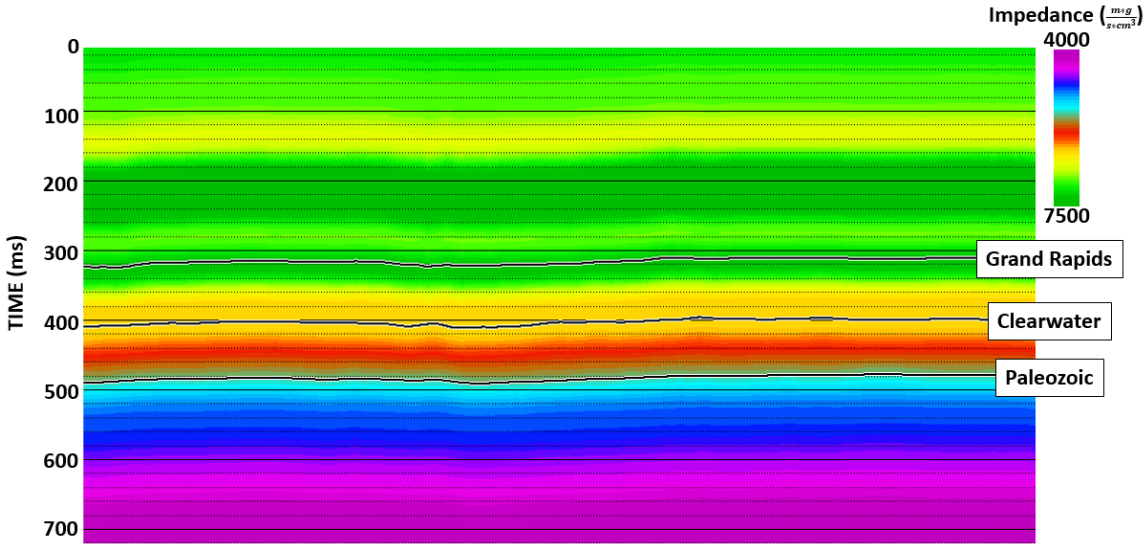

FIG. 39. Input low frequency model for model-based post-stack PP impedance inversion.

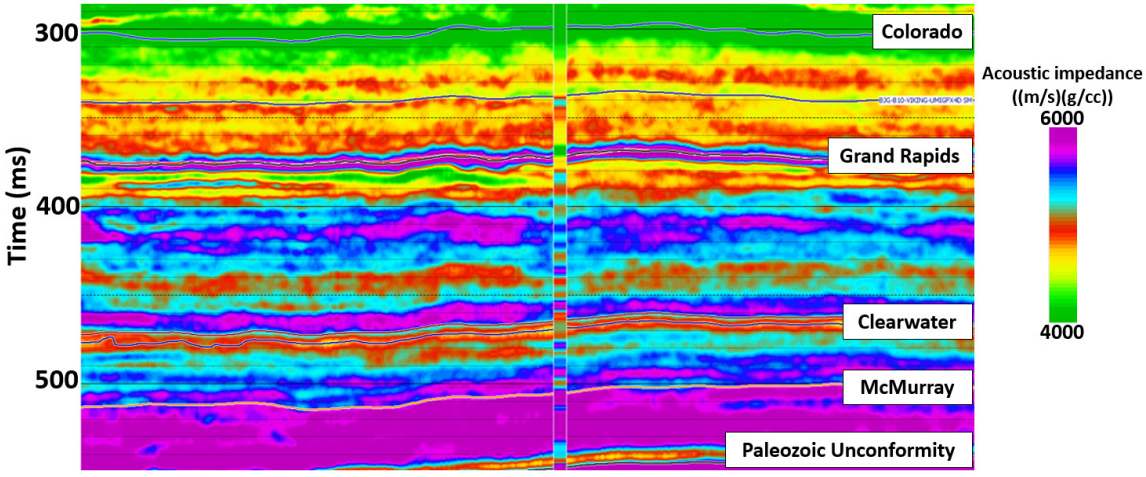

FIG. 40. Impedance inversion cross section with blind well log.

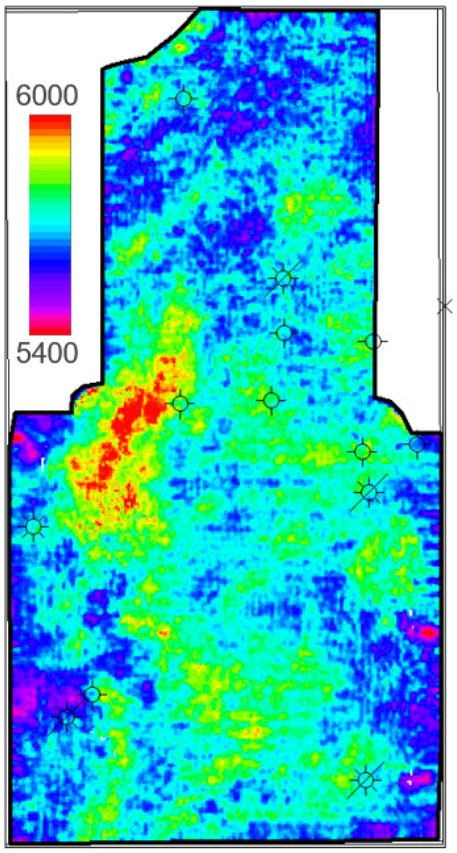

FIG. 41. Upper McMurray RMS impedance and well position for Figure #.

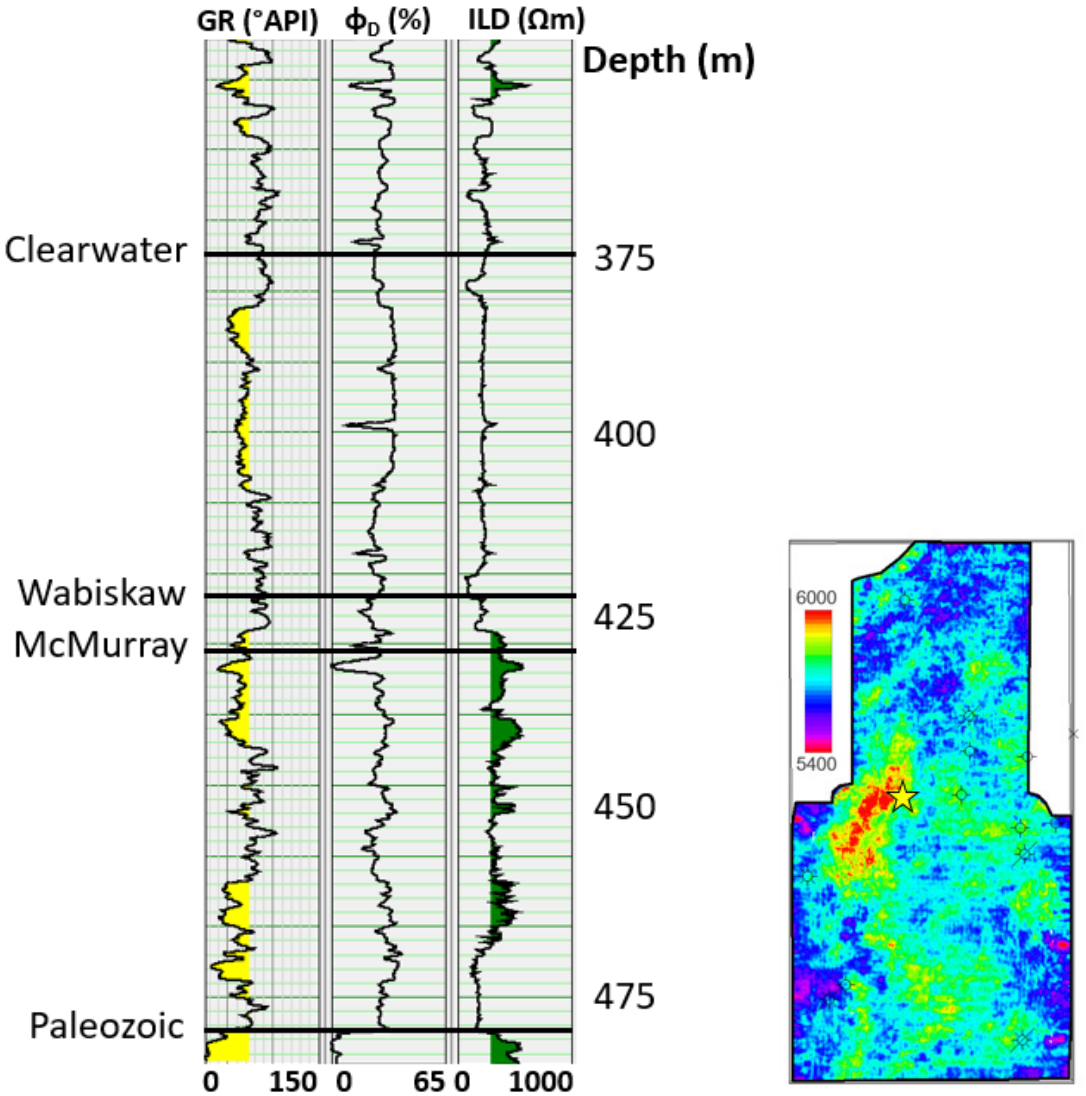

FIG. 42. Well log through region with high RMS impedance in the Upper McMurray Fm. Cleaner reservoir sands are seen in the Upper McMurray Fm; based on the gamma ray log.

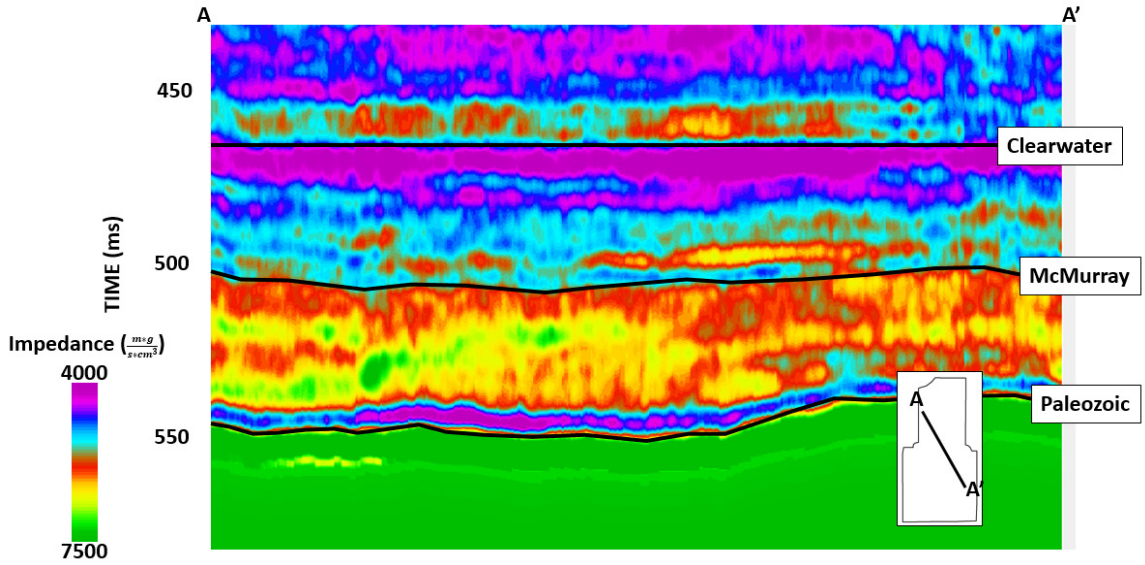

FIG. 43. P impedance cross section through McMurray B2 channel trend – green zones in the McMurray formation likely have the best quality reservoir.

Following the analysis of the post-stack PP impedance inversion, a pre-stack inversion is performed. Pre-stack inversion follows a similar algorithm as post-stack inversion except for a few key processes. In pre-stack inversion, compressional impedance, shear impedance and density are inverted for simultaneously. Using approximation of the Zoeppritz equations, PP and PS reflectivity can be known as a function of angle. Therefore, the input seismic volumes used in pre-stack inversion are angle gathers. In this case, the Aki-Richards equation, a linearized version of the Zoeppritz equations is used as the expression for reflectivity as a function of angle. It is usually necessary to condition pre-stack gathers before attempting a pre-stack inversion. Here, gathers were first organized into super gathers; radon de-noising and trim statics were applied to the super gathers to enhance signal. Example angle gathers are shown in Figure 44. The AVO effects at first glance on the angle gathers are fairly sparse. However, there are definitely AVO effects, particularly in the 450 ms to 480 ms range, which happens to coincide with the McMurray Fm. In addition to utilizing angle gathers, an angle-dependent wavelet is used in the pre-stack inversion process. The angle dependent wavelet is statistically generated using the angle gathers. In a similar fashion to the post-stack inversion, a low frequency model is generated from the regional interpretation and a single well log.

A cross section showing both the post-stack PP impedance inversion and the pre-stack PP impedance inversion is shown in Figure 45. The cross section in Figure 45 intersects the regional McMurray sequence, that is, no large channel features exist in the cross section. The pre-stack inversion results shows better differentiation within the McMurray Formation between sands and shales. A cross section through the McMurray B2 channel trend through the pre-stack PP P-impedance (Figure 46) shows a clear truncation of the regional McMurray sequence. The impedance in the McMurray channel is fairly variable; the highest quality reservoir should correlate with the highest impedance zones. P-impedance volumes are an effective tool in generating lithological models as well. For

example, the McMurray formation top is a marginal reflection horizon on stacked PP seismic data but on the P impedance volumes (Figures 43 and 45) the boundary between the Wabiskaw Member and the McMurray Formation are clear.

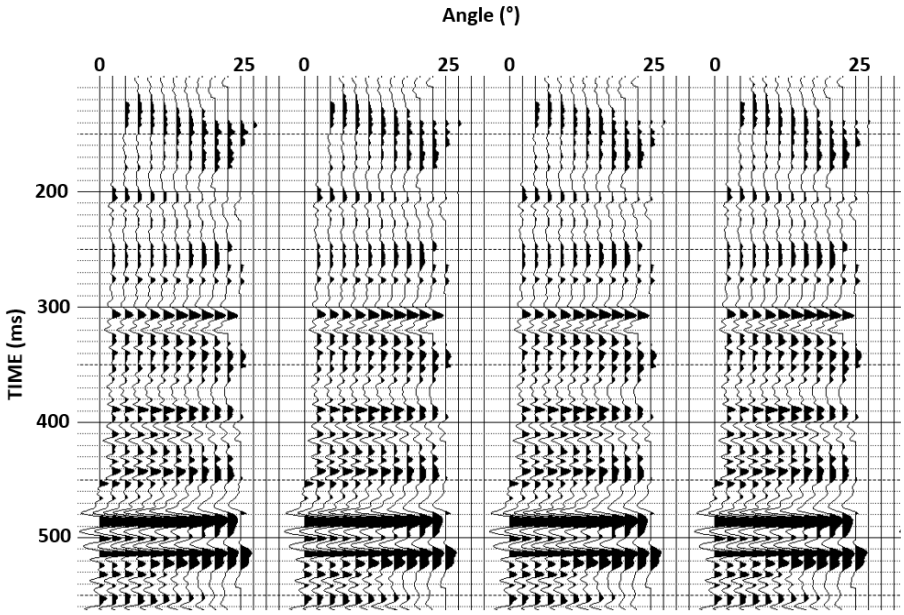

FIG. 44. Conditioned angle gathers, used as input to pre-stack PP migration.

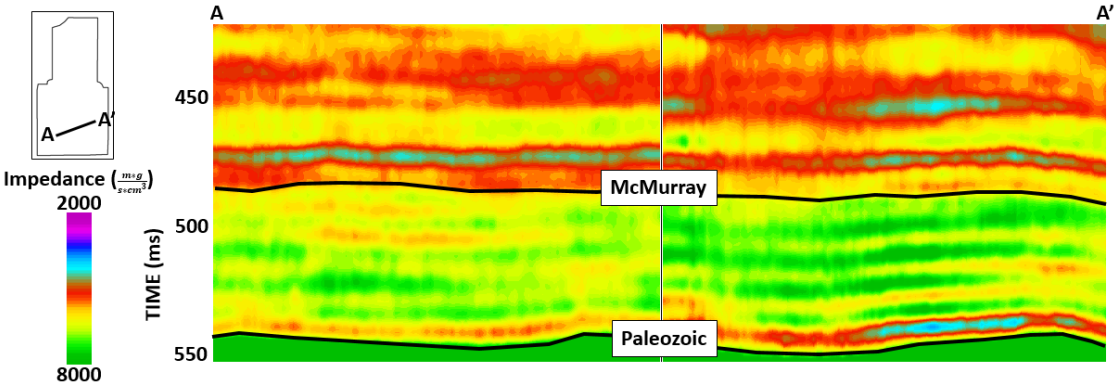

FIG. 45. Cross section comparing post-stack PP inversion (left) and pre-stack PP inversion (right). Regional McMurray package is shown (490-540 ms).

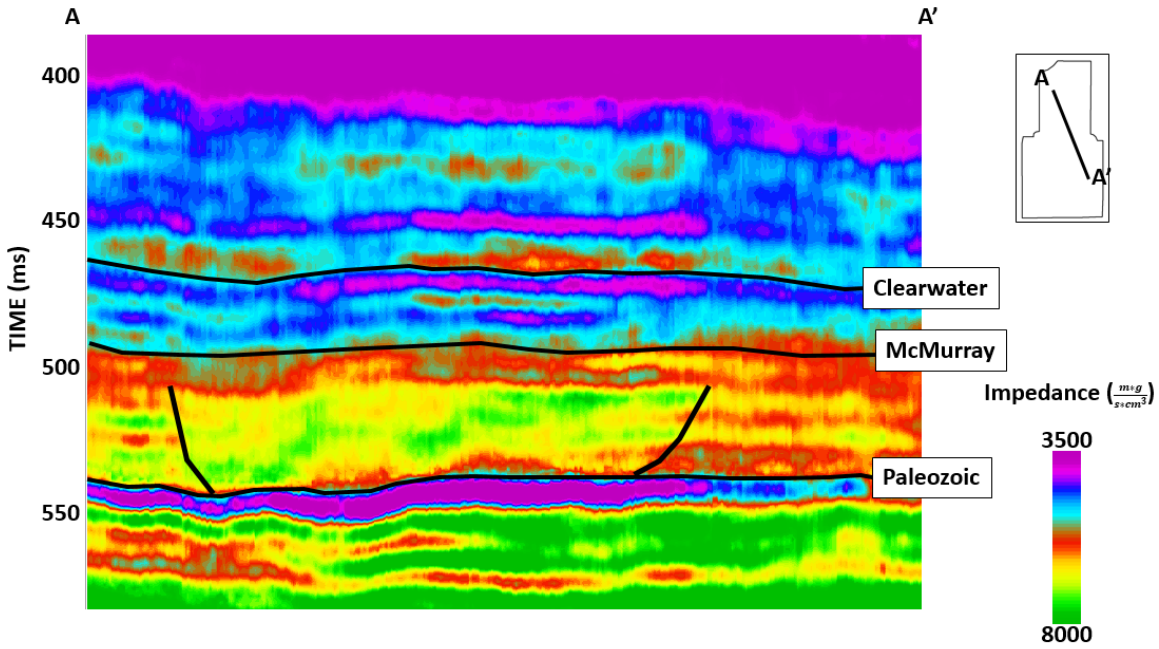

FIG. 46. P-impedance cross section from the PP pre-stack inversion. Truncation of regional McMurray Fm is highlighted. Best channel sands are highest impedance zones within McMurray channel (green).

In addition to generating a second, relatively improved, P-impedance volume a pre-stack inversion creates shear impedance (Figure 47), density (Figure 48) and Vp/Vs (Figure 49) volumes. Blind well crosscorrelation in the zone of interest yield values of 0.66, 0.45 and 0.80 for shear impedance, density and Vp/Vs respectively. These values indicate a reasonable inversion results for shear impedance and Vp/Vs but not for density. These results are expected based on the offset content. Pre-stack inversion for density requires larger offset angles up to 30 degrees. In this survey, offset angles are close to maximum at 25 degrees. Density cannot be reliably determined through pre-stack inversion in this case. To make geological conclusions with the inversion results, interpretation of the pre-stack inversion results should be limited to only the impedance and Vp/Vs volumes. Interval RMS maps, made in a similar fashion to p-impedance interval RMS, can be used in addition to other reservoir studying tools to further delineate subsurface geology. Shear impedance and Vp/Vs interval RMS maps are shown in 50. The McMurray B2 aged channel incision identified through basic seismic maps can further be studied with these physical property maps. The channel feature tends to have lower shear impedance and higher Vp/Vs than the regional McMurray sequence.

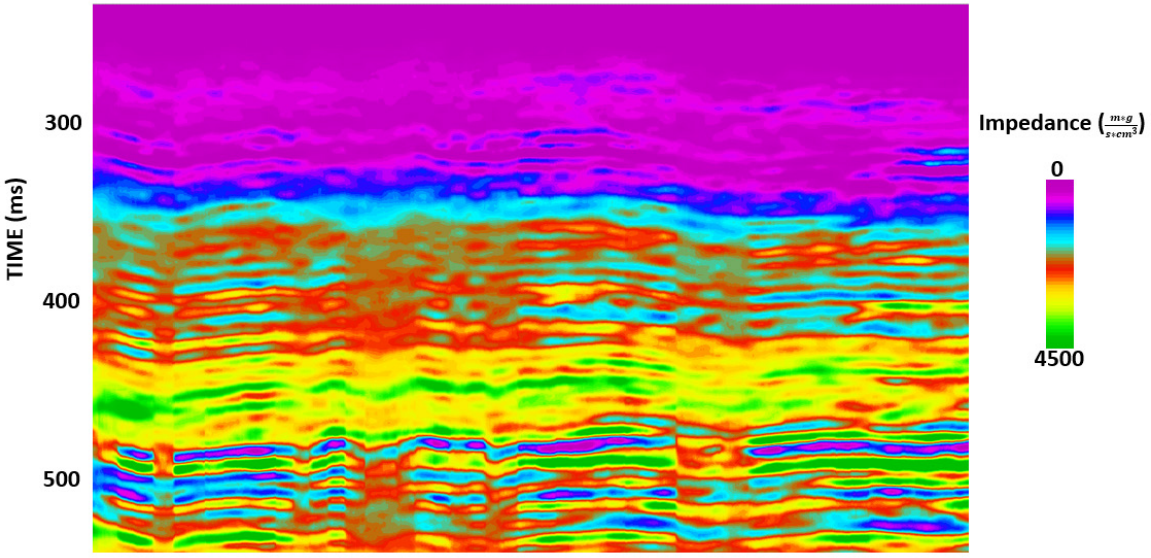

FIG. 47. Shear impedance cross section from pre-stack inversion.

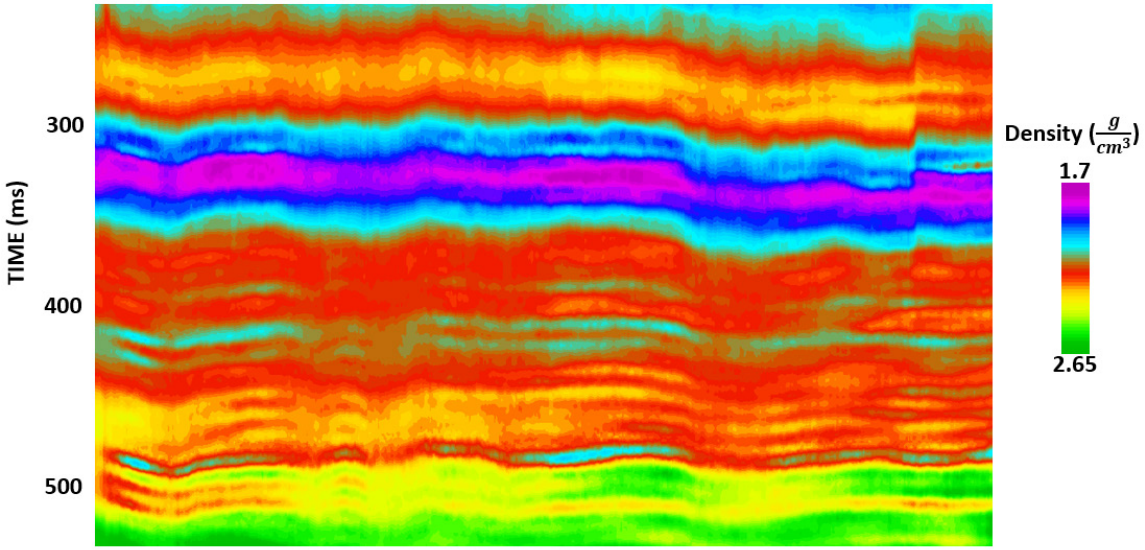

FIG. 48. Density cross section from pre-stack inversion.

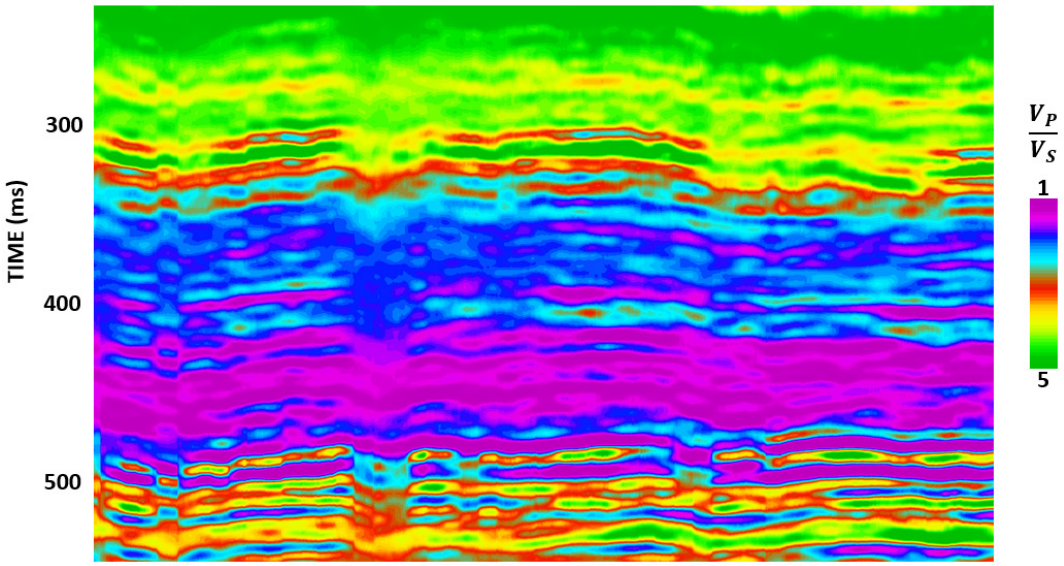

FIG. 49. Vp/Vs cross section from pre-stack inversion.

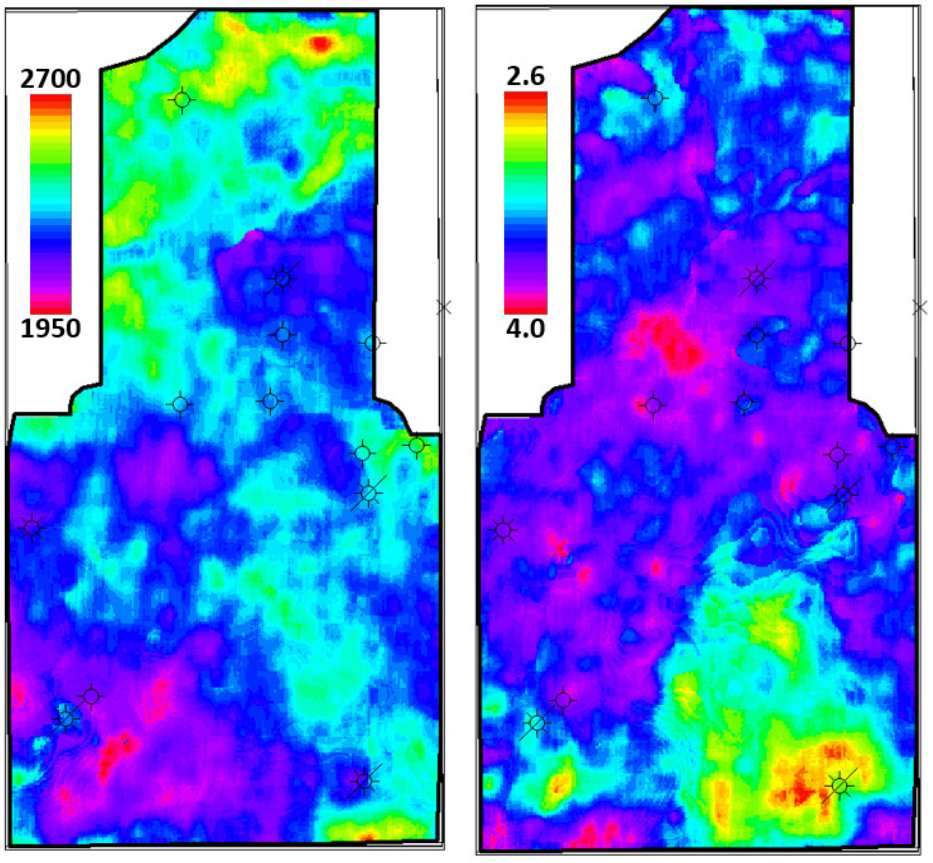

FIG. 50. Interval RMS shear impedance (left) and Vp/Vs (right) for upper McMurray.

CONCLUSIONS AND FUTURE WORK

In this project, a 3C 3D seismic dataset was analyzed. The 3D seismic data was acquired in 2013 in the Athabasca Oil Sands region of Northeast Alberta. The inline and crossline geophone components were rotated into radial and transverse converted wave components. The vertical and radial geophone components were processed into PP and PS staked datasets. PP prestack data was processed and conditioned for prestack inversion. The post stack volumes' regional geology were interpreted based on synthetic seismogram ties to well control. The main geological discontinuities were found to be relatively pervasive reflection horizons on both the PP and PS stacked seismic data. A large incised valley fill of McMurray B2 age was identified from the seismic data. Interval RMS maps based on a model based post stack pp impedance inversion and PP seismic amplitude showed where potential hydrocarbons and porous reservoir were present.

Going forward, there is still much that can be done with the multicomponent seismic dataset used for this project. A PP-PS joint inversion can provide a secondary source of rock property volumes. These joint inversion outputs will be compared to the prestack inversion outputs. Multiattribute analysis has been used to predict well log attributes outside of density, impedance and Vp/Vs. Rops and Lines (2005) made viscosity predictions using multiattribute analysis and Hampson et al., (2001) were able to accurately predict well log properties using least squares minimization and two neural networks. An important next step in this project will be using multiattribute analysis to predict key well log properties such as porosity and gamma ray.

ACKNOWLEDGEMENTS

We would like to thank the data and software providers for this project. Canadian Natural Resources Limited provided the high quality 3C 3D seismic survey used here, for which we are incredibly grateful. Seisware, Hampson-Russel, GeoScout, ProMAX and Vista processing software were used in this project and we thank the companies: Seisware, CGG, GeoLOGIC systems inc., Halliburton and Schlumberger for the use of these software packages. This project is funded by CREWES industrial sponsors and NSERC through grant CRDPJ 461179-13.

REFERENCES

Andriashek, L.D., 2003, Quaternary geological setting of the Athabasca Oil Sands (in situ) area, Northeast Alberta, Alberta Energy and Utilities Board, Alberta Geological Survey

Castagna, J.P., Batzle, M.L., and Eastwood, R.L., 1985, Relationships between compressional-wave and shear-wave velocities in clastic silicate rocks: Geophysics, 50, 571-581

Crude oil forecast, markets & transportation, 2015, Canadian Association of Petroleum Producers

Fenton, M.M., Schreiner, B.T., Nielsen, E., and Pawlowicz, J.G., 1994, Quaternary geology of the western plains: Geological atlas of the Western Canada Sedimentary Basin, Chapter 26

Gingras. M. and Rokosh, D., 2004, A brief overview of the geology of heavy oil, bitumen and oil sand deposits, 2004 CSEG National Convention

Glass, D.J., 2009, Wabiskaw Member, Lexicon of Canadian Stratigraphy, Volume 4, CSPG, Natural Resources Canada

Hayes, B.J.R., Christopher, J.E., Rosenthal, L., Los, G., and McKercher, B., 1994, Cretaceous Mannville Group of the Western Canada Sedimentary Basin: Geological atlas of the Western Canada Sedimentary Basin, Chapter 19

Hampson, D.P., Schuelke, J.S., and Quirein, J.A., 2001, Use of multiattribute transforms to predict log properties from seismic data, Geophysics, Vol 66, No. 1, 220-236

Hampson-Russell, 2013, Emerge: multiattribute analysis [course notes]

Isaac, J.H., 1996, Seismic methods for heavy oil reservoir monitoring, Ph.D. thesis, University of Calgary, Department of Geology and Geophysics

Kelly, B.M., 2012, Processing and interpretation of time-lapse seismic data from a heavy oil field, Alberta, Canada, Ph.D. thesis, University of Calgary, Department of Geology and Geophysics

Krief, M., Garat, J., Stellingwerff, J., and Ventre, J., 1990, A petrophysical interpretation using velocities of P and S waves (full waveform sonic): The Log Analyst, 31, No. 6

Leckie, D.A., Bhattacharya, J.P., Bloch, J., Gilboy C.F., and Norris, B. 1994, Cretaceous Colorado/Alberta Group of the Western Canada Sedimentary Basin: Geological atlas of the Western Canada Sedimentary Basin, Chapter 20

Oldale, H.S., and Munday R.J., 1994, Devonian Beaverhill Lake Group of the Western Canada Sedimentary Basin: Geological atlas of the Western Canada Sedimentary Basin, Chapter 11

Rops, E.A., and Lines, L.L., 2015, Predicting heavy oil viscosity from well logs – testing the idea, CREWES Research Report, Vol. 26, Chapter 65

Schafer, A.W., 1992, A comparison of converted-wave binning methods using a synthetic model of the Highwood Structure, Alberta, CREWES Research Report, 4

Todorivic-Marinic, D., Gray, D., and Dewer, J., 2015, Strategies to fill in the details for an oil sands reservoir: Kinosis example: CSEG Recorder, January 2015, 18-24